Analysis of Lysosomal Enzyme Receptors in Enteric Protozoan Parasite *Entamoeba histolytica*

A Dissertation Submitted to

the Graduate School of Life and Environmental Sciences,

the University of Tsukuba

in Partial Fulfillment of the Requirements

for the Degree of Doctor of Philosophy in Science

(Doctoral Program in Biological Sciences)

Konomi MARUMO

TABLE OF CONTENTS

ABSTRACT

Lysosomes are a degradative organelle in a cell and formed by maturing of endosomes. It is necessary that lysosomal hydrolases are synthesized on the ER, modified on the Golgi apparatus and then targeted into endosomes. In model organisms, it is known that the selective trafficking of lysosomal enzymes from Golgi apparatus to endosomes is achieved by the cargo specific receptors. The absent of hydrolase receptors causes miss secretion of the lysosomal hydrolases out of the cell. Therefore lysosomal enzyme receptor plays a fundamental role in both the biogenesis of lysosomes and secretion of lysosomal hydrolases.

Amoebiasis with dysentery in large intestine (colon), the most frequent protozoan disease in Japan, is caused by *Entamoeba histolytica*. *E. histolytica* also causes the extraintestinal amoebiasis by the achievement of the translocation from colon into the other organ, e.g. liver and brain, through a blood streams. Cysteine proteases (CPs), known to be a virulence factor in *E. histolytica*, are secreted to the intestinal surface and cause the destruction of the host tissue and the activation of host metalloproteases. CPs are also important for *E. histolytica* to digest the materials ingested by phagocytosis. Therefore, elucidation of CP trafficking and secretion mechanisms in *E. histolytica* is important for understanding of amoebic pathogenesis and lysosomal biogenesis. However, in *E. histolytica* genome there are no homologs of the proteins responsible for the lysosomal trafficking in model organisms, such as mannose 6-phosphate receptor, Sortilin and Vps10p. Thus, the lysosomal trafficking mechanism in *E. histolytica* is still unclear.

Previously, cysteine protease binding protein family (CPBF) 1 was identified as the receptor of CP-A5 and also its family proteins were found. CPBF1 is involved in the trafficking and the processing of CP-A5. While CPBF6 and CPBF8 are related to phagosomal trafficking of α-amylase and γ-amylase or lysozyme and β-hexosaminidase, respectively. However, for other CPBF proteins, their ligands, binding specificity and binding mechanisms are unclear, and thus their roles in the CP trafficking are still unknown.

In order to better understand the functions of CPBF proteins, I established *E. histolytica* transformants expressing CPBF2, 3, 4, 5, 7, 9, 10 and 11, tagged with the carboxyl-terminal hemagglutinin (HA) epitope and identified the binding proteins by immunoprecipitation using anti-HA antibody and liquid chromatography tandem-mass spectrometry (LC-MS/MS) analysis. CPBF2, 7 and 10 were shown to be associated to α-amylase1, two β-hexosaminidases, and α-amylase2 and 3, respectively. While, for CPBF3, 4, 5, 9 and 11, no ligands were identified. I also examined the localization of these CPBF-HA proteins by immunofluorescence assay. CPBF3, 4 and 11 were localized on ER-like small vesicles. CPBF2, 7, 9 and 10 were localized on ER-like vesicles and partially on lysosomal membrane like structure stained by LysoTracker. CPBF5 also localized on the ER-like vesicles, and colocalized with LysoTracker, suggesting the localization inside of the lysosomes. Hence, these CPBF proteins localized basically on ER, while CPBF2, 7, 9 and 10 also localized on the lysosomal membrane. Whereas, CPBF5 localized inside of the lysosomes.

On the other hand, to elucidate the site of ligand recognition in CPBF, I developed the

recombinant CPBF1 protein with bacterial prepeptidase carboxyl-terminal domain (PPC) like-domain and examined the association of these recombinants with endogeneous CP-A5 using pull-down assay. As a result, it was found that the among the six PPC domains, domain 3 dominantly bound to CP-A5.

Next, to understand the relationship of CPBF with amoebic pathogenicity, I established the *cpbf*-gene silenced strains using the small RNA mediated transcriptional gene silencing system. For these strains, I conducted the screening to identify the CPBF which is related to the amoebic virulence by *in vitro* Matrigel invasion assay. In this experiment, *cpbf2*-silenced strain showed significant defect in Matrigel invasion. To confirm whether α-amylase was related to this phenotype, I also examined the Matrigel invasion ability of (CPBF2 ligand) α-*amylase1*- and other two α-*amylase*-gene-silenced strain. Compared with a mock control strain, the ability was not changed. Additionally, intracellular and secreted amylase activities of *cpbf2*-silenced strain or α-*amylase*-silenced strain were not different from those of control strain. Therefore, α-amylase was not involved in the defect of Matrigel invasion in *cpbf2*-silenced strain. I also examined another phenotype of *cpbf2*-silenced strain. Since in *cpbf2*-silenced strain, adhesion to collagen coated plate was increased, I tried to assess the cell motility of *cpbf2*-silenced strain. I tracked the cell movement from live imaging data taken by a confocal microscopy. *Cpbf2*-silenced strain showed very slow motility compared with the control strain. Thus, the facilitation of adhesion and the defect of Matrigel invasion in *cpbf2*-silenced strain were likely caused by low motility. Finally, I performed the RNA-seq

analysis for *cpbf2*-silenced strain. Expression of 77 genes in total were two-fold changed compared with those of wild-type strain. Among these genes, ten genes, including serine palmitoyltransferase, Rab7F and AIG1 family protein, etc., were upregulated, while sixty seven genes, including cytoskeleton related, regulation of gene expression and membrane trafficking, etc., were downregulated.

In this study, it was revealed that eleven *Entamoeba* CPBF proteins recognized their specific ligands, and localized to different sites in the cell. From the examination of the recombinants, it was suggested that PPC-like domain was ligand recognition unit. Different from the generally accepted molecular mechanism that lysosomal enzymes are recognized by their ligands depending on the specific sugar modifications, *Entamoeba* CPBF proteins are likely to directly recognize each ligand protein. It is needed to elucidate how each CPBF protein has ligand specificity with the same domain composition.

Cpbf2-silenced strain showed the significant defect of Matrigel invasion. It was suggested that CPBF2 plays a pivotal role in amoebic virulence. α-amylase, the ligand of CPBF2, was reported to increase in its transcription level depending on the extent of attachment with human colon, and thus was expected to be related to amoebic invasion. In the present study, however, I could not directly demonstrate the evidence for the relationship of α-amylase with amoebic invasion. If α-amylase was actually related to invasion, CPBF2 would have another function different from lysosomal enzymes receptor. *Cpbf2*-silenced strain showed the enhanced adherence to collagen and the very slow cell motility. Since the cell motility is

involved in the amoebic invasion, the defect of Matrigel invasion in *cpbf2*-silenced strain is plausibly caused by the low motility. In the transcriptome analysis of *cpbf2*-silenced strain, expression of some cytoskeleton related genes and cytoskeletal regulatory genes were reduced. Although the molecular mechanism of the regulation is still unclear, it was found that CPBF2 regulated the amoebic cell motility.

GENERAL INTRODUCTION

Lysosomal biogenesis and enzyme receptor

Lysosomes are membrane-bound organelles and serve as a site for delivery of materials targeted for degradation within the central vacuolar system of eukaryotic cells. In this role, lysosomes are placed as the route of many endocytic, autophagic and secretory materials for degradation (Luzio, *et al.*, 2007). Lysosomal degradation is important for many physiological processes, including the turnover of normal cellular proteins, removal of abnormal organelle, down-regulation of surface receptors, release of endocytosed nutrients, inactivation of pathogenic organisms and antigen processing (Mizushima, *et al.*, 2008; Kaushik and Cuervo, 2012; Luzio, *et al.*, 2009). In addition, lysosomes play pivotal roles in metal ion homeostasis and plasma membrane repair (Polishchuk and Polishchuk, 2016; Settembre, *et al.*, 2013). Lysosomes are containing many hydrolytic enzymes which are active on an acidic environment. The lysosomal membrane consists a single bilayer lipid membrane and contains proteins which are involved in transport of substances into an out of the lumen, acidification of the lysosomal lumen and fusion of the lysosome with other membrane structures (Saftig and Klumperman, 2009). Lysosomal maturation is accomplished by traffic through early endosomes to late endosomes/multivesicular bodies (Luzio, *et al.*, 2014), and by delivery of lysosomal hydrolases and complete fusions between late endosomes and lysosomes.

Lysosomal hydrolases are synthesized in the endoplasmic reticulum (ER) and pass through

the Golgi apparatus then sorted to the lysosomes in a receptor mediated manner. In mammals, majority of the lysosomal hydrolases are modified with mannose 6-phosphate (M6P) and two types of M6P receptors, cation dependent (CD-) and cation independent (CI-) M6P receptors, recognize M6P in the Golgi and target them to the endosome/lysosome system (Coutinho, *et al.*, 2012). There are also several M6P-independent trafficking receptors are known such as Sortilin, LIMP2, LDLR, LRP1, LRP2, SEZ6L2 and MRC1 (Staudt, *et al.*, 2016). M6P receptors and M6P-independent receptors consist of variety of proteins. M6P receptor and MRC1 recognize carbohydrate modification on the cargo with lectin domain. Sortilin has Vps10p domain forming β-propeller fold and the cavity between the blades is involved in cargo recognition. LDLR, LRP1 and LRP2 share LDLR repeats and LIMP2 and SEZ6L2 have unique structures. LRP1 binds to the Cathepsin D through the β chain of the extracellular domain. LIMP2 interacts with β-glucocerebrosidase via a coiled-coil domain within the luminal domain.

Entamoeba histolytica

Entamoeba histolytica is the agent of amoebiasis, which is the second leading cause of death due to parasitic disease in the world (Stanley, 2003). *E. histolytica* infects an estimated 50 million people, resulting in 40,000-100,000 deaths annually (Ximénez, *et al.*, 2009). Trophozoites colonizing the large intestine produce watery and bloody diarrhea (Haque, *et al.*, 2003). In some cases, they also migrate to blood stream and reached the other organs,

resulting in the extraintestinal amoebiasis (Grecu, *et al.*, 2006). In intestinal lumen, trophozoites secrete an abundant cysteine protease (CP) that can degrade colonic mucin barrier (Moncada, *et al.*, 2006) and extracellular matrix (ECM) (Que and Reed, 2000) to invade and damage the host tissues. First step of invasion for the intestinal wall is contact with and degradation of mucus layer to allow the trophozoites to attach the epithelial surface. Next is closely adhesion of the amoeba to the mucosal cells inducing the expression of its cytolytic activity. And then, *E. histolytica* induce a host inflammatory response, achieving the intestinal infection.

Lysosomal enzyme receptors in *E. histolytica*

Lysosomal enzymes such as CPs play a pivotal role in the pathogenesis of the intestinal parasitic protist *E. histolytica*. Cytolytic capacity and tissue invasiveness of this parasite are mainly attributed to CPs, as shown in numerous *in vitro* and *in vivo* studies (Brinen *et al.*, 2000; Que and Reed, 2000; Hellberg *et al.*, 2001, 2002; Bruchhaus *et al.*, 2003; Que *et al.*, 2003; Ackers and Mirelman, 2006; Gilchrist *et al.*, 2006; MacFarlane and Singh, 2006; Meléndez-López *et al.*, 2007; He *et al.*, 2010; Ralston and Petri, 2011). The regulation of their intracellular processing and transport has begun to be unveiled by a recent discovery of the novel CP-specific carrier/receptor protein, named cysteine protease binding protein family (CPBF) 1 (Nakada-Tsukui *et al.*, 2012). CPBF1 is a unique cargo receptor restricted to the Amoebozoa, and shows a number of differences from known transport receptors in

other eukaryotic lineages. As describe above, model organisms in Opisthoconta, mammals and yeast, have MPR, Sortilin/Vps10p controls. And also, it is known that there are Chloroplastida and Excavata specific receptors, plant specific valuolar sorting receptor (VSR) and *Giardia lamblia* specific vacuolar protein sorting (GlVps). There are two genes encoding putative CD-MPR in *E. histolytica*. However, immunoprecipitation of influenza virus hemagglutinin (HA)-tagged CD-MPRs demonstrated no interaction with soluble lysosomal proteins (Nakada-Tsukui *et al*., unpublished data), suggesting that MPRs are unlikely to function as lysosomal targeting receptors in *E. histolytica*. Furthermore, neither Sortilin/Vps10p, VSR, nor GlVps is present in the genome.

The purpose of this study

CPBF is unique lysosomal receptor/transporter and forms eleven family proteins in *E. histolytica*, which different with other lysosomal enzyme receptors. It is already known that CPBF1, 6 and 8 regulate the trafficking of hydrolases, including CP, lysozymes and β-hexosaminidases. However, the function of other CPBF proteins are still unknown. The purpose of this study is understanding of the unique mechanisms of lysosomal biogenesis and trafficking in *E. histolytica* through the elucidation of the CPBF functions. It will make clear a part of the mechanism of virulence mechanisms of *E. histolytica*.

PART1. CYSTEINE PROTEASE BINDING PROTEIN FAMILY IN *E. HISTOLYTICA*

1.1. Introduction

Lysosomal enzymes such as cysteine proteases (CPs) play a pivotal role in the pathogenesis of the intestinal parasitic protist *E. histolytica*. The regulation of their intracellular processing and transport has begun to be unveiled by a recent discovery of the novel CP-specific carrier/receptor protein, named cysteine protease binding protein family (CPBF) 1 (Nakada-Tsukui *et al.*, 2012). CPBF1 is a unique cargo receptor restricted to the Amoebozoa.

In *E. histolytica*, CPBF consists of 11 members with 18–75% mutual amino acid identities. Previously, it was demonstrated that three most highly expressed CPBF proteins, CPBF1, 6 and 8 are involved in the targeting of soluble lysosomal proteins including CP, amylases, β-hexosaminidase and lysozymes (Furukawa *et al.,* 2012, 2013; Nakada-Tsukui *et al.,* 2012). As MPR, Sortilin/Vps10p and VSR are generally encoded by a single gene in the genome, CPBF represents the first protein family involved in targeting of lysosomal enzymes. All members of CPBF proteins share similar features such as the signal sequence at the amino terminus, a single transmembrane domain and the YxxΦ motif at the carboxyl terminus. The YxxΦ motif (Y is tyrosine, x is any amino acid and Φ is any aliphatic amino acid) is known to be present in the cytoplasmic portion of numerous receptors and responsible for binding to the adaptor protein (AP) complex (Nakatsu and Ohno, 2003). These common features suggest that all members of CPBF are involved in lysosomal targeting of respective specific

soluble lysosomal proteins.

The structures of CPBF proteins were predicted using FORTE (Tomii and Akiyama, 2004), which performs profile-profile alignments for protein structure prediction, by Dr. Tomii (AIST, Japan). FORTE allowed me to identify five PPC (bacterial prepeptidase carboxyl-terminal domain)-like domains at the luminal portion of each CPBF. PPC family (Pfam ID: PF04151) (Punta *et al*., 2012) includes a large and diverse set of protein domains that possess two β-sheets. The PPC domains are typically located at the carboxyl-termini of secreted proteases and may be involved in their secretion and/or localization (Yeats *et al*., 2003). By manual inspection and sequence alignment, I identified an additional PPC-like domain, D4, which was not inferred by FORTE. There are similarities between individual PPC-like domains of each CPBF protein. I identified conserved cysteines and aromatic/hydrophobic residues in the predicted β-strands of the six PPC-like domains of CPBF1. Similarly, it appears that all CPBF proteins contain a region consisting of six PPC-like domains in the luminal portion.

To further examine the specificity and heterogeneity of the ligands of other members of CPBF proteins, I attempted to identify and characterize the ligands for CPBF2, 3, 4, 5, 7, 9, 10 and 11 by immunoprecipitation and mass spectrometric analysis and to elucidate the function of PPC domain in CPBF by *in vitro* binding assay using recombinant PPC domains.

1.2. Materials and methods

1.2.1. Cell culture

Trophozoites of *E. histolytica* strain HM-1:IMSS cl6 (HM-1) (Diamond *et al.,* 1972) were cultured axenically in BI-S-33 medium (Diamond *et al.,* 1978) at 35.5 °C as previously described (Clark and Diamond, 2002). Amoeba transformants were cultured in the presence of 10 μg/mL of Geneticin (Invitrogen). *Escherichia coli* strain DH5α was purchased from Life Technologies (Tokyo, Japan). All chemicals of analytical grade were purchased from Sigma–Aldrich (Tokyo, Japan) unless otherwise stated.

1.2.2. Plasmid construction

Standard techniques were used for routine DNA manipulation, subcloning and plasmid construction (Sambrook and Russell, 2001). Plasmids to express CPBF2, 3, 4, 5, 7, 9, 10 or 11 fused with the HA epitope at the carboxyl terminus were generated by the insertion of the corresponding protein coding region of the *cpbf*-gene into the *Bgl*II site of a pEhExHA vector (Nakada-Tsukui, *et al.,* 2009) either by standard restriction digestion and ligation methods for CPBF3, 4, 10 and 11, or by In-Fusion system (Takara, Tokyo, Japan) for CPBF2, 5, 7 and 9. The resultant plasmids were named pEhExHA-CPBF2, 3, 4, 5, 7, 9, 10 and 11. The protein coding region of each *cpbf*-gene was amplified with specific sense and antisense oligonucleotide primers:

5'-acacattaacAGATCATGGTTGTTCTGTTTTTATT-3' and

5’-atggatacatAGATCGAAAGTTCCAAATGATGATT-3’ (CPBF2);

5’-accggatccATGATCCTATTAATTCTAGCA-3’ and

5’-gttggatccAAGTTCATGATATCCCAAAAA-3’ (CPBF3);

5’-accggatccATGGTCCAAATAACATGTCTT-3’ and

5’-gttggatccAAGTTCATGATATCTCAATAA-3’ (CPBF4);

5’-acacattaacAGATCATGTTTATTCTTCTTAGTCT-3’ and

5’-atggatacatAGATCAAAGTCAGAATAACTCTTTC-3’ (CPBF5); 5’-acacattaac

AGATCATGTTGGTTTTCTTAACAAT-3’ and 5’-atggatacatAGATCAACTAAA

GTAGCATATCCAG-3’ (CPBF7);

5’-acacattaacAGATCATGTTATTGAAATGGGGATT-3’ and

5’-atggatacatAGATCATTATCAATAATTGTTTTTA-3’ (CPBF9);

5’-accggatccATGCTTTTAATAACTCTCCTC-3’ and

5’-gttggatccGAAACTACTGAAACTTGATGA-3’ (CPBF10);

5’-accggatccATGTTTTTGTTGTTCATTTCT-3’ and

5’-gttggatccTAATTCATAATATCCTTTGTT-3’ (CPBF11). Plasmids to express GST-fusion proteins with the individual PPC domain (PPC1-6) of CPBF1 were generated by the insertion of the synthesized nucleotides corresponding to CPBF1 PPC1-6 or the first PPC domain of CPBF8 (CPBF8 PPC1) into the *Bam*HI and *Not*I double-digested pGEX6p-2 vector (GE Healthcare, Tokyo, Japan), and designated as pGST-CPBF1 PPC1-6 or pGST-CPBF8 PPC1, respectively. CPBF1 PPC1-6 corresponds with amino

acids (a.a.) 20-165, 172-298, 303-428, 435-570, 574-710 and 717-853, of CPBF1, respectively, and CPBF8 PPC1 corresponds to a.a. 16-154 of CPBF8.

1.2.3. Amoeba transfection

pEhExHA-CPBF2, 3, 4, 5, 7, 9, 10 or 11 was introduced into HM-1 trophozoites by lipofection, as previously described (Nozaki *et al.,* 1999). Geneticin was added at a concentration of 1 μg/mL at 24 h after transfection and gradually increased for approximately 2 weeks until the concentration reached 10 μg/mL.

1.2.4. Immunoprecipitation, SDS–PAGE and immunoblot analysis

For the isolation of CPBF-HA binding proteins, the cell pellet from 2.0×10^7 CPBF-HA-expressing or mock-transfected cells was lysed with 1 mL of lysis buffer (50 mM Tris–HCl pH 7.5, 150 mM NaCl, 1% Triton-X100, 0.5 mg/mL of E-64 and complete mini EDTA-free protease inhibitor cocktail (Roche Applied Science, Penzberg, Germany)). After centrifugation at 14,000 × g for 5 min at 4 °C, the soluble lysate was pre-cleared with 50 μL of protein G Sepharose (50% slurry in lysis buffer), (GE Healthcare, Waukesha, WI, USA) and then mixed and incubated with 50 μL of anti-HA monoclonal antibody-conjugated agarose (Sigma–Aldrich, St. Louis, MO, USA) for 3.5 h at 4 °C. Immune complexes bound to the resin were washed five times with wash buffer (50 mM Tris–HCl pH 7.5, 150 mM NaCl, 1% Triton-X100) and then eluted by incubating the resin with 180 μL of 200 mg/mL HA peptide (Sigma–Aldrich) in lysis buffer for 16 h at 4 °C. Approximately 2 μg of the

eluted samples were subjected to SDS–PAGE and visualised with either a silver stain MS kit (WAKO, Tokyo, Japan) or a SYPRO ruby protein stain (Takara). The same samples were also subjected to SDS–PAGE and immunoblot analyses as previously described (Sambrook and Russell, 2001). Primary antibodies were used at a 1:500 dilution for anti-Cm-CP-A5 rabbit antibody (Nakada-Tsukui *et al.,* 2012) or at a 1:1000 dilution for anti-HA mouse monoclonal antibody (clone 11MO, Covance, Princeton, NJ, USA) in immunoblot analyses.

1.2.5. Mass spectrometric analysis

Unique bands detected exclusively in the eluted samples from the HA-tagged transformants but not those from the control, after visualisation by silver or SYPRO ruby stain, were excised and subjected to LC-MS/MS analysis. The total mixture of the immunoprecipitated eluates using the lysate from CPBF2, 3, 4, 5, 7, 9, 10 and 11-HA expressing and mock transformants were briefly electrophoresed on SDS–PAGE to allow entry of proteins into the gel, visualized by silver stain, and the bands containing whole mixture were excised and subjected to LC–MS/MS analysis. LC–MS/MS analysis was performed at W. M. Keck Biomedical Mass Spectrometry Laboratory, University of Virginia, USA. The gel pieces from the band were transferred to a siliconized tube and washed in 200 µL of 50% methanol. The gel pieces were dehydrated in acetonitrile, rehydrated in 30 µL of 10 mM DTT in 0.1 M ammonium bicarbonate and reduced at room temperature for 0.5 h. The DTT solution was removed and the sample alkylated in 30 µL of 50 mM iodoacetamide

in 0.1 M ammonium bicarbonate at room temperature for 0.5 h. The reagent was removed and the gel pieces dehydrated in 100 μL of acetonitrile. The acetonitrile was removed and the gel pieces rehydrated in 100 μL of 0.1 M ammonium bicarbonate. The pieces were dehydrated in 100 μL of acetonitrile, the acetonitrile removed and the pieces completely dried by vacuum centrifugation. The gel pieces were rehydrated in 20 ng/μL of trypsin in 50 mM ammonium bicarbonate on ice for 30 min. Any excess enzyme solution was removed and 20 μL of 50 mM ammonium bicarbonate added. The sample was digested overnight at 37 °C and the peptides formed extracted from the polyacrylamide in a 100 μL aliquot of 50% acetonitrile/5% formic acid. This extract was evaporated to 15 μL for MS analysis. The LC–MS system consisted of a Thermo Electron Velos Orbitrap ETD mass spectrometer system with a Protana nanospray ion sourceinterfaced to a self-packed 8 cm x 75 μm inner diameter Phenomenex Jupiter 10 μm C18 reversed-phase capillary column. The extract (7 μL) was injected and the peptides eluted from the column by an acetonitrile/0.1 M acetic acid gradient at a flow rate of 0.5 μL/min over 1.2 h. The nanospray ion source was operated at 2.5 kV. The digest was analyzed using the double play capability of the instrument, acquiring a full scan mass spectrum to determine peptide molecular weights followed by product ion spectra to determine a.a. sequence in sequential scans.

1.2.6. Data analysis to determine specific binding proteins

The data were analyzed by database searching using the Sequest search algorithm against

the *E. histolytica* genome database (http://amoebadb.org/amoeba/). The quantitative value (QV), normalized with unweighted spectrum counts, was used to estimate relative quantities of proteins in the samples. Specific binding proteins were determined by the following criteria. First, proteins that showed QV > 8, or QV > 10 in the control pEhExHA transformed sample ("HA" in Table 2) and proteins that showed QV < 3 in the CPBF samples were removed, and it was assumed that those were non-specific proteins. The proteins that showed >3 or >4-fold higher QV in the CPBF samples compared with those in the HA control were selected. Finally, proteins lacking the signal sequence were removed from a list of possible ligands. Applying these criteria to the proteins discovered, positive controls, i.e., CPs in CPBF1-HA, were unequivocally detected.

1.2.7. Indirect immunofluorescence assay

The indirect immunofluorescence assay was performed as previously described (Nakada-Tsukui *et al.,* 2012). Briefly, the amoeba transformant cells were harvested and transferred to 8 mm round wells on a slide glass, and then fixed with 3.7% paraformaldehyde in PBS, pH 7.2, for 10 min. After washing, the cells were permeabilized with 0.2% saponin in PBS containing 1% BSA for 10 min, and reacted with an anti-HA monoclonal antibody (clone 11MO, Covance) diluted at 1:1000 in PBS containing 0.2% saponin and 1% BSA. After washing three times with PBS containing 0.1% BSA, the samples were then reacted with Alexa Fluor 488-conjugated anti-mouse secondary antibody (1:1000 dilution in PBS

containing 0.2% saponin and 1% BSA) for 1 h. For lysosomal staining, 10 μM Lysotracker Red (Molecular Probes, Eugene, OR, USA) was added to *E. histolytica* transformants for 16 h, and the trophozoites were then washed, harvested and subjected to an immunofluorescence assay. The samples were examined on a Carl-Zeiss LSM 510 META confocal laser-scanning microscope. The resultant images were further analyzed using LSM510 software.

1.2.8. Recombinant protein expression and *in vitro* binding assay

GST-fused recombinant proteins containing individual PPC domains (CPBF1 PPC1-6 and CPBF8 PPC1) were produced as follows: pGST-CPBF1PPC1-6 and pGST-CPBF8PPC1 were introduced into *E. coli* BL21(DE3) competent cells (Merck, Tokyo, Japan). Expression of the recombinant proteins was induced with 100 mM isopropyl-β-thiogalactoside (IPTG) at 25 °C for 5 h. The bacterial cells were collected and lysed by adding bacterial protein extraction reagent in phosphate buffer (B-PER) (Thermo Scientific, Tokyo, Japan) to the cell pellet. Clear lysate was mixed with glutathione Sepharose 4B (GE Healthcare) for 1 h at 4 °C and then washed three times with wash buffer (50 mM Tris–HCl pH 7.5, 150 mM NaCl, 1% Triton-X100). The GST-CPBF PPC-bound Sepharose beads were mixed with the soluble supernatant of lysates prepared from 3×10^6 HM-1 trophozoites as described in Immunoprecipitation, SDS–PAGE and immunoblot analysis and incubated for 1 h at 4 °C. The beads were washed three times with wash buffer and boiled with SDS–PAGE loading buffer. The eluted proteins were separated by SDS–

PAGE and analyzed by Coomassie Brilliant Blue stain (CBB, one step CBB stain kit, Bio Craft, Tokyo, Japan) and an immunoblot assay. Images of CBB-stained polyacrylamide gel and immunoblots were acquired by GELSCAN (iMeasure Inc., Nagano, Japan) and LAS3000 (GE Healthcare), respectively. The O.D. of the bands was quantified using Image J (http://rsbweb.nih.gov/ij/index.html). Binding efficiency was estimated with the parameter defined as the O.D. of the band corresponding to CP-A5 on an immunoblot divided by the O.D. of the GST-fusion protein band on a CBB-stained gel. Relative binding efficiency of each GST-PPC domain fusion protein to CP-A5 was expressed after normalization against the value of the GST control.

1.3. Results and discussion

1.3.1. Establishment of CPBF-HA over expressing transformants

While the ligands of CPBF1, 6 and 8 were identified in the previous studies (Furukawa *et al.,* 2012, 2013; Nakada-Tsukui *et al.,* 2012), the spectrum of the ligands recognized by other members of CPBF proteins remained poorly understood. Thus, I established *E. histolytica* transformants expressing CPBF2, 3, 4, 5, 7, 9, 10 or 11, tagged with the carboxyl-terminal HA epitope, to identify the ligands of all members of CPBF proteins. In all experiments, the amoeba transformants transfected with a pEhExHA mock vector and a pCPBF1-HA vector were used as negative and positive controls respectively. Expression of HA-fused CPBF proteins was confirmed by immunoblot analysis with anti-HA antibody (Fig. 1). All of the

HA-tagged CPBF proteins showed molecular masses slightly higher than those predicted, as seen for other HA-tagged proteins (Nakada-Tsukui *et al.,* 2005, 2012; Furukawa *et al.,* 2012, 2013). Even if considering the effect of the HA tag, CPBF7 and CPBF10 showed higher molecular masses than other CPBF proteins, suggesting possible post-translational modifications, similar to CPBF6 and CPBF8 which have a serine-rich region (SRR) upstream of the transmembrane domain (Furukawa *et al.,* 2012, 2013). It was previously demonstrated that a deletion of the SRR in CPBF8 caused a mobility shift in the predicted molecular masses and a decrease in the ligand binding (Furukawa *et al.,* 2012). In addition, CPBF7 and CPBF10 showed a close kinship with CPBF6 and CPBF8 by a phylogenetic analysis (Nakada-Tsukui *et al.,* 2012). While CPBF7 has a SRR (Furukawa *et al.,* 2012), there is no apparent SRR in CPBF10; CPBF10 contains only two serine residues within the luminal portion near the transmembrane domain. There is no potential N-glycosylation site, either, as predicted by NetNglyc 1.0 server (http://www.cbs.dtu.dk/services/NetNGlyc/).

1.3.2. Immunoprecipitation of CPBF-binding proteins

All CPBF-HA- and mock-transfected *E. histolytica* lines were subjected to immunoprecipitation with anti-HA antibody, separated by SDS-PAGE and visualized with silver or SYPRO ruby stain (Fig. 2). Immunoprecipitation of the CPBF-HA proteins was confirmed in all transformants. Compared with the mock transfected line ("HA" in Fig. 2), one extra band at approximately 70 kDa in CPBF2-HA, and three extra bands at

approximately 60, 55 and 40 kDa in CPBF10-HA, and one extra band around 45 kDa in CPBF11-HA were detected (Fig. 2B and C). These specific bands were excised and subjected to LC-MS/MS analysis. I also analyzed whole immunoprecipitated samples from lysates of CPBF1, 2, 3, 4, 5, 7, 9, 10, 11 and the mock control by LC-MS/MS. In the following sections, I categorized CPBF members based on their ligand specificities.

1.3.3. CPBF2, CPBF6 and CPBF10 bound to amylases

Three CPBF proteins, namely CPBF2 and CPBF10, as well as previously identified CPBF6 (Furukawa *et al.,* 2013), bound to a variety of amylases. Silver staining of immunoprecipitated samples from CPBF2-HA lysates after SDS–PAGE showed a specific 70 kDa band (Fig. 2C). LC–MS/MS analysis of the band (Table 1) and the whole immunoprecipitated sample (Table 2) indicated the protein to be α-amylase (XP_655699, EHI_152880), with 22% and 42% coverage, respectively, and a high QV (122.5 for the whole sample). The 60 and 55 kDa bands exclusively detected in CPBF10-HA were identified as α-amylases (XP_655636 (EHI_023360) and XP_656406 (EHI_153100)), with 23% and 25% coverage, respectively (Table 3). These two amylases were also detected in the whole immunoprecipitated sample from CPBF10-HA (Table 2). One should note that these two α-amylases were different from α-amylases that bind to CPBF2 (XP_655699, EHI_152880). The 40 kDa band detected in the immunoprecipitated sample from CPBF10-HA was not unequivocally assigned (QV < 4). Another α-amylase, XP_656406 (EHI_153100), was

detected from the 40 kDa band, despite a low QV (3) and being more frequently detected in the 55 kDa band. Intriguingly, one α-amylase (XP_655636, EHI_023360) was also identified as the cargo of CPBF6 (Furukawa *et al.,* 2013), which shows phylogenetic kinship with CPBF10 (Nakada-Tsukui *et al.,* 2012). In addition to these α-amylases, β-amylase, XP_653896 (EHI_192590), was detected from whole mixture. Three α-amylases found as CPBF ligands in this study were previously detected in the phagosome proteome studies (Okada *et al.,* 2006; Furukawa *et al.,* 2013). A recent transcriptomic analysis using the *ex vivo* human colon explant showed that trophozoites of the virulent strain showed a remarkable up-regulation of genes implicated in carbohydrate metabolism and processing of glycosylated residues compared with the non-virulent strain (Thibeaux *et al.,* 2013). It was shown in that among the carbohydrate metabolism-related genes, β-amylase (XP_653896, EHI_192590) was the most highly induced (approximately 17-fold increase) in the virulent strain compared with the non-virulent strain. Furthermore, Thibeaux *et. al.* (2013) showed that the gene repression of β-amylase caused a reduction in mucus layer degradation. Together with the previous observation of β-amylase localization in phagosomes (Furukawa *et al.,* 2013), these findings suggest a role for amylases and their corresponding CPBF receptors in pathogenesis.

1.3.4. Polymorphism of amylases

There are at least five independent (non-allelic) *α-amylase*-genes (XP_656406, EHI_153100; XP_655636, EHI_023360; XP_655699, EHI_152880; XP_649162,

EHI_130690; XP_652044, EHI_055650). Among these five α-amylases, CPBF2, 6 and 10 bind to three of them (XP_656406, EHI_153100; XP_655636, EHI_023360; and XP_655699, EHI_152880), all of which possess the signal peptide. Among α-amylases that interact with CPBF proteins, XP_655699 (EHI_152880) and XP_656406 (EHI_153100) specifically interact with CPBF2 and CPBF10, respectively, whereas XP_655636 (EHI_023360) interacts with both CPBF6 and CPBF10. XP_655636 (EHI_023360) is the most highly expressed mRNA among all putative *α-amylase*-genes, as demonstrated by the previous microarray analysis (Penuliar *et al.,* 2012). This is one of the two examples in which one ligand is recognized by more than one CPBF proteins (see below). Although it was previously shown that SRR is essential for the binding of CPBF6 to α- and γ-amylases (Furukawa *et al.,* 2013), CPBF10 appears to lack SRR. Possible post-translational modifications on CPBF10, as suggested by slower migration on SDS–PAGE (see Section 1.3.1), and their involvement in the ligand interaction needs to be investigated.

1.3.5. CPBF7 bound to β-hexosaminidase, similar to CPBF8, amoebapore and MPR

Three possible lysosomal luminal proteins, two β-hexosaminidases (XP_656208 (EHI_012010) and XP_650273 (EHI_007330)) and an amoebapore B precursor, were detected in the whole immunoprecipitated sample from CPBF7-HA (Table 2), while those were not detectable by SDS–PAGE and silver staining (Fig. 2C). The *E. histolytica* genome encodes three β-hexosaminidases, two of which were bound to CPBF7-HA, and the other,

AJ582954 (XP_657529, EHI_148130), was recognized by CPBF8 (Furukawa *et al.,* 2012, Table 1). It was shown that this β-hexosaminidase (AJ582954) is localized in cytoplasmic granules and phagosomes (Riekenberg *et al.,* 2004; Furukawa *et al.,* 2012) and all three β-hexosaminidases have the signal peptide. Thus, unlike amylases, all β-hexosaminidases seem to be carried by CPBF proteins. Both CPBF7 and CPBF8 have SRR, which was shown to be essential for β-hexosaminidase binding by CPBF8 (Furukawa *et al.,* 2012). β-hexosaminidases are involved in the hydrolysis of terminal N-acetyl-D-hexosamine residues in hexosaminides. When *E. histolytica* trophozoites propagate extraintestinally, they take a route similar to that during metastasis of cancer cells (Leroy *et al.,* 1995), which requires both proteases and glycosidases during the passage of the basement membrane (Bernacki *et al.,* 1985; Liotta, 1984). Furthermore, it was shown that β-hexosaminidase activity is involved in mucin degradation (Stewart-Tull *et al.,* 1986). β-hexosaminidase was found as one of the transcriptionally upregulated genes after *E. histolytica* trophozoite's contact with human colon epithelia in an *ex vivo* model (Thibeaux *et al.,* 2013). Taken together, β-hexosaminidases and their traffic regulation are important for the pathogenesis of *E. histolytica*. Identification of amoebapore B precursor as a CPBF7 cargo is important as amoebapores are described as major virulence factors (Leippe *et al.,* 2005). Amoebapores are the cytolytic peptides homologous to granulysin, which is present in human cytotoxic lymphocytes, displays potent cytolytic activity towards bacterial and human cells, and forms ion channels in artificial membranes (Leippe, 1997). Amoebapores are targeted to lysosomes

and mainly involved in degradation of ingested bacteria. Inhibition of expression of the amoebapore A gene by antisense or gene silencing caused a reduction in virulence, suggesting that this protein plays a key role in pathogenesis (Bracha *et al.,* 1999, 2003). One of two MPRs in *E. histolytica*, MPR1, was also found as a CPBF7-binding protein. MPR1 is predicted to have a single CRD, but the a.a. residues implicated for mannose 6-phosphate binding (Dahms *et al.,* 2008) are not conserved. Immunoprecipitation and LC-MS/MS analysis of HA-tagged MPR1 was performed, but failed to identify the ligand (personal communication from Dr. Nakada-Tsukui, data not shown). It is of note that in *Saccharomyces cerevisiae* Vps10p and a single CRD domain-containing protein, Mrl1p (Whyte and Munro, 2001), cooperatively function in the traffic of lysosomal (vacuole in yeast) proteins, but no ligand was assigned for Mrl1p. It is plausible that MPR1 and CPBF7 are cooperatively involved in trafficking to lysosomes.

1.3.6. CPBF9 bound to lysozyme, similar to CPBF8

Lysozyme 2, XP_656933 (EHI_096570), was found to bind to CPBF9-HA (Table 2), however, no specific bands were detect by SDS–PAGE or silver staining (Fig. 2C). It has previously been shown that lysozyme 2 is also recognized by CPBF8 (Furukawa *et al.,* 2012). Lysozymes are encoded by six independent genes in the *E. histolytica* genome and annotated as lysozymes or N-acetylmuraminidase. Among them, the *lysozyme 2*-gene is the most highly transcribed (Penuliar *et al.,* 2012). Lysozymes are well-known glycosidases that degrade the

bacterial cell wall (Chipman *et al.,* 1967). It was reported that *lysozyme*-genes were poorly expressed in an avirulent *E. histolytica* Rahman strain and in *Entamoeba dispar* (MacFarlane and Singh, 2006; Davis *et al.,* 2007). Furthermore, expression of *lysozyme*-genes was repressed when *E. histolytica* trophozoites were treated with 5-azacytidine, a potent inhibitor of DNA methyltransferase, and the repression of *lysozyme*-genes correlated with a reduction in virulence (Ali *et al.,* 2008). It was also demonstrated that repression of *cpbf8*-gene expression by small antisense RNA-mediated transcriptional silencing (Bracha *et al.,* 1999, 2003) caused a decrease in the targeting of lysozyme 2 to phagosomes and delay in digestion of ingested gram-positive bacteria (Furukawa *et al.,* 2012). It was also reported that the SRR of CPBF8 is glycosylated and glycosylation is important for the binding of β-hexosaminidase and lysozyme 2 (Furukawa *et al.,* 2012). CPBF9 has no SRR, and does not seem to have post-translational modifications. These data indicate that mechanisms of interaction between CPBF9 and lysozyme 2 must be different from those of CPBF8 and lysozyme 2.

1.3.7. Identification of additional CPBF1 binding proteins

To further identify additional lysosomal proteins recognized by CPBF1 other than previously identified CPs, I vigorously searched for other binding proteins. Based on the criteria described in Section 1.2.6, the proteins identified in four independent experiments and those repeatedly detected (either in two, three or four out of the four experiments) are listed (Table 4). I detected a total of 20 proteins in the four experiments. Among them, four

proteins were detected in all four experiments (CP-A2, CP-A4, CP-A5 and CPBF1 itself), while three other proteins were detected in two or three experiments. CP-A1 and CP-A6 were detected only in a single experiment (Table 4). None of the possible soluble lysosomal proteins, other than CPs, were detected as CPBF1-HA binding protein, reinforcing the specificity of CPBF1 to CPs and verifying the stringency of the protocol used in the study. Previous study identified CP-A1 as one of the cargos for CPBF1 by a pull-down experiment of CPBF1-HA, followed by immunoblot analysis using anti-CP-A1 antibody (Nakada-Tsukui *et al.,* 2012). One should note that anti-CP-A1 antibody cross-reacted with CP-A2 due to the high a.a. identity (81%) (Mitra *et al.,* 2007). In the present study, LC–MS/MS data have clearly shown that CPBF1 preferentially interacts with CP-A2 but not CP-A1. CP-A1 and CP-A2 are the two major CPs with comparably high expression levels, followed by CP-A5 in *E. histolytica* HM-1:IMSS (Tillack *et al.,* 2007). CP-A4 is one of the poorly expressed CPs, but suggested to be involved in the pathogenesis of invasive amebiasis (Tillack *et al.,* 2007; He *et al.,* 2010). Reproducible detection of CP-A4 in all of the experiments indicates the high affinity of CPBF1 toward CP-A4. Interestingly, CP-A4 is localized to the nuclear region and the acidic compartment (He *et al.,* 2010). The role of CPBF1 in the CP-A4 localization needs to be elucidated. As more than 95% of the CP activity of *E. histolytica* trophozoites is attributed to CP-A1, A2, A5 and A7 (Bruchhaus *et al.,* 2003; Irmer *et al.,* 2009), the amounts of CPs bound to CPBF1 does not seem to be proportional to their expression levels, but determined by the ligand specificity of CPBF1. I

reproducibly identified heat shock protein 70 (Hsp70) (XP_654737, EHI_199590), which has the ER retention signal (KDEL) at the carboxyl terminus (three out of four experiments). It is worth noting that this protein was repeatedly detected in all immunoprecipitation experiments except for CPBF4. Mannosyltransferase, localized in the ER (Maeda and Kinoshita, 2008; Loibl and Strahl, 2013), was also repeatedly identified (two out of four experiments). Identification of the ER-residing Hsp70 and mannosyltransferase suggests possible involvement of ER proteins in the functionality of CPBF1. Hypothetical protein (XP_649888, EHI_146110), with no detectable domain or motif, was detected in two out of four experiments.

1.3.8. Analysis of ligands for CPBF3, CPBF4, CPBF5 and CPBF11

No known or possible hydrolases or membrane proteins were detected either by SDS–PAGE analysis followed by silver staining or LC–MS/MS analysis of the whole immunoprecipitated samples, with a few exceptions: CP-A2 and a light subunit of galactose/N-acetylgalactosamine-inhibitable lectin in CPBF4-HA (with low QV, 3.44) (Fig. 2A, Table 2). Thus, no specific ligand was identified for CPBF4. It may be worth noting that the pIs of CPBF3, CPBF4, CPBF11 (7.2, 6.5 and 6.5, respectively) are higher than those of other members; the average pI value of the 11 CPBF proteins is 5.5. CPBF3 was detected by immunoprecipitation of CPBF4-HA and vice versa. CPBF3 and CPBF4 have high mutual a.a. identity (75%, Table 6). Three peptides detected in the CPBF3-HA pull-down sample

were mapped to CPBF4 (5% coverage). Similarly, five peptides were mapped to CPBF3 in the CPBF4-HA pull-down sample (7% coverage). These data indicate interaction between CPBF3 and CPBF4. Serine threonine isoleucine rich protein (STIRP) was found in the immunoprecipitated sample from CPBF4-HA. Another isotype of STIRP (XP_656227.2, EHI_012330) was also detected, although it was removed from Table 2 due to lack of the signal peptide. Since the carboxyl-terminal regions of these proteins show high mutual similarity (MacFarlane and Singh, 2007), detected peptides did not differentiate two EhSTIRPs. EhSTIRP, which contains a single transmembrane domain, was exclusively expressed in virulent *E. histolytica* strains, but not in non-virulent *E. histolytica* Rahman strain or *E. dispar*, and thus is considered to be a virulent associated protein (MacFarlane and Singh, 2007). Possible interaction between STIRP and CPBF4 needs to be further verified. A light subunit of galactose/N-acetylgalactosamine-inhibitable lectin was found in the immunoprecipitated sample from CPBF4-HA and CPBF5-HA. It is well established that this lectin is involved in the interaction between *E. histolytica* and host cells/microbes, and is essential for pathogenesis (Ravdin *et al.,* 1989; Petri *et al.,* 2002). The lectin is composed of three subunits, i.e. heavy, intermediate and light subunits (Petri *et al.,* 2002). The 170 kDa heavy subunit with a transmembrane domain and the 31–35 kDa glycosylphosphatidylinositol (GPI)-anchored light subunit form a heterodimer by disulfide bonds. An intermediate subunit of 150 kDa is non-covalently associated with the heterodimer. All three subunits are encoded by multigene families. There are five genes for

the heavy subunit, six to seven for the light subunit and 30 for the intermediate subunit (Petri *et al.,* 2002). The fact that only specific light subunits were associated with CPBF4 and CPBF5, respectively, indicates that these light subunits together with the corresponding CPBF proteins may be involved in trafficking of the surface receptor in association with other lysosomal receptors. CPBF5 was found to also interact with two additional proteins, neither of which seems to be a potential lysosomal protein. Interestingly, an immunofluorescence assay (Fig. 3D, see Section 1.3.9) showed that CPBF5-HA is localized in lysosomes, as indicated by colocalization with LysoTracker. This is in good contrast with other CPBF proteins mainly localized in the ER/Golgi compartments, e.g., CPBF1, CPBF6 and CPBF8. Assuming that the receptor binds to the ligand depend on pH, as shown for CPBF1 (Nakada-Tsukui *et al.,* 2012), the conditions for pull-down experiments may need to be further optimized to obtain the ligand of CPBF5. A 45 kDa band was specifically detected in the immunoprecipitated sample from CPBF11-HA by SYPRO ruby stain (Fig. 2C), but identified as CPFB11 itself by LC-MS/MS analysis (Table 7). The whole immunoprecipitated sample was subjected to MS analysis, but no additional binding protein was detected (Table 2). It is worth noting that mRNA expression of a gene encoding a CPBF11 homologue in *Entamoeba invadens*, a reptilian sibling of *E. histolytica* and the model of encystation, is 4.7–9-fold upregulated after 24–120 h of encystation (De Cádiz *et al.,* 2013). The finding may explain why no CPBF11 ligand was discovered in trophozoites. Identification of CPBF11 binding proteins from *E. histolytica* cysts may be needed.

1.3.9. Intracellular localization of CPBF proteins

Intracellular localization of CPBF proteins was examined by immunofluorescence assay with anti-HA antibody using LysoTracker stained trophozoites of CPBF-HA-expressing lines (Fig. 3). CPBF2, 7, 9 and 10-HA were detected on vacuolar membranes and small membrane structures scattered all over the cells. CPBF3, 4 and 11 were mostly localized on small membrane structures and hardly detected on vacuolar membranes. In contrast, as briefly mentioned 1.3.8, CPBF5-HA was nicely colocalized with LysoTracker, indicating lysosomal localization. However, CPBF5 was not identified in previous phagosome proteome study (Okada *et al.,* 2006; Furukawa *et al.,* 2012), which may be due to low expression of endogenous CPBF5. Partial colocalization was also observed for CPBF2, 7, 9 and 10. Localization of the CPBF proteins involved in the transport of carbohydrate digesting enzymes, CPBF2, CPBF7 and CPBF10, was similar to that of CPBF6 and CPBF8 (Furukawa *et al.,* 2012, 2013). They are localized on both the vacuolar membrane and the small membrane structures. It was previously shown that CPBF6 and CPBF8 are colocalized with pyridine nucleotide transhydrogenase (PNT), which utilizes the electrochemical proton gradient across the membrane to drive NADPH formation from NADH (Yousuf *et al.,* 2010).

1.3.10. PPC domain is a functional unit of the ligand binding of CPBF1

To investigate whether the binding activity of CPBF1 to CP can be attributable to specific

PPC domain(s), each PPC domain, CPBF1 domains 1–6 (D1–D6), was expressed as GST-fusion protein in *E. coli*, with CPBF8 domain 1 (D1) as negative control and an *in vitro* pull-down assay was performed (Fig. 4). Among the six PPC domains of CPBF1, D3 showed significantly higher affinity ($P < 0.05$) compared with D1 and D6 (Fig. 4C). D5 also showed significantly higher affinity than D6 ($P < 0.05$). These results indicate that single PPC domains per se have the ability of ligand binding. D4 was truncated or degraded during expression and/or purification and not used in the study. The mechanisms of ligand recognition of CPBF proteins have not been elucidated. Previously, it was showed that carbohydrate modifications of SRR are involved in ligand binding of CPBF6 and CPBF8 (Furukawa *et al.*, 2012, 2013). However, only CPBF6-8 apparently have SRR, whereas other CPBF proteins lack it.

A phylogenetic analysis of six PPC-like domains of 11 CPBF proteins indicates that corresponding domains (e.g., D3) of all CPBF proteins tend to form clusters (data not shown). This likely implies, together with the fact that all CPBF proteins have similar domain configuration, that individual corresponding domains (e.g., D3, D5) retain distinct structural role(s).

Further structural studies are required to better understand the mechanisms of ligand recognition binding and dissociation, as well as ligand specificities.

GENERAL CONCLUSIONS AND PERSPECTIVES

Lysosomal enzymes play a pivotal role in *E. histolytica* pathogenesis. CPBF regulates these functions through the trafficking of them. CPBF1 transports CP-A5 from ER to lysosomes and control the processing of CP-A5. CPBF6 and CPBF8 is involved in the trafficking of carbohydrolases to phagosomes.

In this study, I identified the ligands of CPBF2, 7, 9 and 10. They bind to carbohydrolases, α-amylases, β-hexosaminidases and lysozymes specifically. Since these CPBF proteins localized on the lysosomal membranes, it seemed that these ligand enzymes functioned at lysosomes. This sort of lysosomal trafficking system which is regulated by diverse family proteins is completely different from already-known mechanisms such as MPR dependent or independent trafficking system in other organisms. In that manner, single receptor protein can recognize and bind to various cargo proteins through the sugar modification or protein conformation. While in *E. histolytica*, CPBF diversifies eleven family proteins, and each CPBF proteins associates with specific ligand proteins. CPBF1 specifically associate with CP-A5 via PPC domain independent of protein modification. Additionally, *E. histolytica* conserved the highly divergent Rab GTPase genes (Nakada-Tsukui *et al.*, 2010), which is related for many membrane trafficking system, suggesting that membrane trafficking system has been evolved uniquely and divergently on the line leading to *E. histolytica*.

The ligand proteins of CPBF3, 4, 5 and 11 could not be identified in this study. To reveal the functions of these CPBF proteins, other approach is needed, such as the

immunoprecipitation with cross-linker or some stimulation, including contact with mammalian cells or host organs and oxidative or starvation stress.

ACKNOWLEDGMENTS

I would like to express my deepest gratitude to my supervisor, Dr. Kumiko Nakada-Tsukui (National Institute of Infectious Disease) and Dr. Tomoyoshi Nozaki (University of Tokyo) for constant guidance, critical advice and comments throughout this study. I also would like to express my appreciation to Dr. Yumiko Nakano-Saito (National Institute of Infectious Disease), Dr. Kisaburo Nagamune (National Institute of Infectious Disease), Dr. Watanabe (University of Tokyo), Dr. Tetsuo Hashimoto (University of Tsukuba) and Dr. Yuji Inagaki (University of Tsukuba) for appropriate comments and advice. I thank all the laboratory members of the University of Tokyo and National Institute of Infectious Disease for valuable comments, discussions and encouragement.

I wish to express my special gratitude to Prof. Naoko Watanabe (Toho University) for giving me to opportunity to carry out his study and various support.

Further, I would like to thank Dr. Kentaro Tomii (National Institute of Standards and Technology) for the *in silico* prediction and analysis.

Finally, I would like to thank my family who provided me with support throughout my life in general.

REFERENCES

Ackers J.P., Mirelman D., 2006. Progress in research on *Entamoeba histolytica* pathogenesis. Curr. Opin. Microbiol. 9, 367-373.

Aguilar-Rojas A., Olivo-Marin J.C., Guillén N., 2016. The motility of *Entamoeba histolytica*: finding ways to understand intestinal amoebiasis. Curr. Opin. Microbiol. 34, 24-30.

Ali I.K.M., Ehrenkaufer G.M., Hackney J.A., Singh U., 2008. Growth of the protozoan parasite *Entamoeba histolytica* in 5-azacytidine has limited effects on parasite gene expression. BMC Genomics 8, 7.

Bernacki R.J., Niedbala M.J., Korytnyk W., 1985. Glycosidases in cancer and invasion. Cancer Metastasis Rev. 4, 81-101.

Biller L., Matthiesen J., Kühne V., Lotter H., Handal G., Nozaki T., Saito-Nakano Y., Schümann M., Roeder T., Tannich E., Krause E., Bruchhaus I., 2014. The cell surface proteome of *Entamoeba histolytica*. Mol. Cell. Proteomics 13, 132-144.

Bosch D.E., Kimple A.J., Muller R.E., Giguère P.M., Machius M., Willard F.S., Temple B.R., Siderovski D.P., 2012. Heterotrimeric G-protein signaling is critical to pathogenic processes in *Entamoeba histolytica*. PLoS Pathog. 8, e1003040.

Bracha R., Nuchamowitz Y., Anbar M., Mirelman D., 2006. Transcriptional silencing of multiple genes in trophozoites of *Entamoeba histolytica*. PLoS Pathog. 2, e48.

Bracha R., Nuchamowitz Y., Leippe M., Mirelman D., 1999. Antisense inhibition of

amoebapore expression in *Entamoeba histolytica* causes a decrease in amoebic virulence. Mol. Microbiol. 34, 463-472.

Bracha R., Nuchamowitz Y., Mirelman D., 2003. Transcriptional silencing of an amoebapore gene in *Entamoeba histolytica*: molecular analysis and effect on pathogenicity. Eukaryot. Cell 2, 295-305.

Brinen L.S., Que X., McKerrow J.H., Reed S.L., 2000. Homology modeling of *Entamoeba histolytica* cysteine proteinases reveals the basis for cathepsin L-like structure with cathepsin B-like specificity. Arch. Med. Res. 31, S63-S64.

Bruchhaus I., Loftus B.J., Hall N., Tannich E., 2003. The intestinal protozoan parasite *Entamoeba histolytica* contains 20 cysteine protease genes, of which only a small subset is expressed during in vitro cultivation. Eukaryot. Cell 2, 501-509.

Chipman D.M., Grisaro V., Sharon N., 1967. The binding of oligosaccharides containing N-acetylglucosamine and N-acetylmuramic acid to lysozyme. J. Biol. Chem. 242, 4388-4394.

Clark C.G., Diamond L.S., 2002. Methods for cultivation of luminal parasitic protists of clinical importance. Clin. Microbiol. Rev. 15, 329-341.

Coudrier E., Amblard F., Zimmer C., Roux P., Olivo-Marin J.C., Rigothier M.C., Guillén N., 2005. Myosin II and the Gal-GalNAc lectin play a crucial role in tissue invasion by *Entamoeba histolytica*. Cell. Microbiol. 7, 19-27.

Coutinho M.F., Prata M.J., Alves S., 2012. Mannose-6-phosphate pathway: a review on its

role in lysosomal function and dysfunction. Mol. Genet. Metab. 105, 542-50.

Dahms N.M., Olson L.J., Kim J.J., 2008. Strategies for carbohydrate recognition by the mannose 6-phosphate receptors. Glycobiology 18, 664-678.

Davis P.H., Scholze J., Stanley Jr. S.L., 2007. Transcriptomic comparison of two *Entamoeba histolytica* strains with defined virulence phenotypes identifies new virulence factor candidates and key differences in the expression patterns of cysteine proteases, lectin light chains, and calmodulin. Mol. Biochem. Parasitol. 151, 118-128.

De Cadiz A.E., Jeelani G., Nakada-Tsukui K., Caler E., Nozaki T., 2013. Transcriptome analysis of encystation in *Entamoeba invadens*. PLoS One 8, e74840.

De la Cruz O.H., Muñiz-Lino M., Guillén N., Weber C., Marchat L.A., López-Rosas I., Ruíz-García E., Astudillo-de la Vega H., Fuentes-Mera L., Álvarez-Sánchez E., Mendoza-Hernández G., López-Camarillo C., 2014. Proteomic profiling reveals that EhPC4 transcription factor induces cell migration through up-regulation of the 16-kDa actin-binding protein EhABP16 in *Entamoeba histolytica*. J. Proteomics 111, 46-58.

Dennis P.A., Rifkin D.B., 1991. Cellular activation of latent transforming growth factor β requires binding to the cation-independent mannose 6-phosphate/insulin-like growth factor type II receptor. Proc. Natl. Acad. Sci. USA 15, 580-584.

Diamond L.S., Harlow D.R., Cunnick C.C., 1978. A new medium for the axenic cultivation of *Entamoeba histolytica* and other *Entamoeba*. Trans. R. Soc. Trop. Med. Hyg. 72, 431-432.

Diamond L.S., Mattern C.F., Bartgis I.L., 1972. Viruses of *Entamoeba histolytica*. I. Identification of transmissible virus-like agents. J. Virol. 9, 326-341.

Furukawa A., Nakada-Tsukui K., Nozaki T., 2012. Novel transmembrane receptor involved in phagosome transport of lysozymes and β-hexosaminidase in the enteric protozoan *Entamoeba histolytica*. PLoS Pathog. 8, e1002539.

Furukawa A., Nakada-Tsukui K., Nozaki T., 2013. Cysteine protease-binding protein family 6 mediates the trafficking of amylases to phagosomes in the enteric protozoan *Entamoeba histolytica*. Infect. Immun. 81, 1820-1829.

Gary-Bobo M., Nirdé P., Jeanjean A., Morère A., Garcia M., 2007. Mannose 6-phosphate receptor targeting and its applications in human diseases. Curr. Med. Chem. 14, 2945-2953.

Gilchrist C.A., Baba D.J., Zhang Y., Crasta O., Evans C., Caler E., Sobral B.W., Bousquet C.B., Leo M., Hochreiter A., Connell S.K., Mann B.J., Petri W.A., 2008. Targets of the *Entamoeba histolytica* transcription factor URE3-BP. PLoS Negl. Trop. Dis. 2008, 2, e282.

Gilchrist C.A., Houpt E., Trapaidze N., Fei Z., Crasta O., Asgharpour A., Evans C., Martino-Catt S., Baba D.J., Stroup S., Hamano S., Ehrenkaufer G., Okada M., Singh U., Nozaki T., Mann B.J., Petri Jr. W.A., 2006. Impact of intestinal colonization and invasion on the *Entamoeba histolytica* transcriptome. Mol. Biochem. Parasitol. 147, 163-176.

Giménez-Scherer J.A., Noriega R., Rico G., Merchant M.T., Kretschmer R.R., 1997. The ultrastructure of *Entamoeba histolytica* locomotion. Arch. Med. Res. 27, 311-318.

Grecu F., Bulgariu T., Blanaru O., Dragomir C., Lunca C., Stratan I., Manciuc C., Luca V. 2006. Invasive amebiasis. Chirurgia 101, 539-542.

Hanadate Y., Saito-Nakano Y., Nakada-Tsukui K., Nozaki T., 2016. Endoplasmic reticulum-resident Rab8A GTPase is involved in phagocytosis in the protozoan parasite *Entamoeba histolytica*. Cell. Microbiol. 18, 1358-1373.

Haque R., Huston C.D., Hughes M., Houpt E., Petri W.A. Jr. 2003. Amebiasis. N. Engl. J. Med. 17, 1565-1573.

He C., Nora G.P., Schneider E.L., Kerr I.D., Hansell E., Hirata K., Gonzalez D., Sajidm M., Boyd S.E., Hruz P., Cobo E.R., Le C., Liu W-T., Eckmann L., Dorrestein P.C., Houpt E.R., Brinen L.S., Craik C.S., Roush W.R., McKerrow J., Reed S.L., 2010. A novel Entamoeba histolytica cysteine proteinase, EhCP4, is key for invasive amebiasis and a therapeutic target. J. Biol. Chem. 285, 18516-18527.

Hellberg A., Nickel R., Lotter H., Tannich E., Bruchhaus I., 2001. Overexpression of cysteine proteinase 2 in *Entamoeba histolytica* or *Entamoeba dispar* increases amoeba-induced monolayer destruction *in vitro* but does not augment amoebic liver abscess formation in gerbils. Cell. Microbiol. 3, 13-20.

Hellberg A., Nowak N., Leippe M., Tannich E., Bruchhaus I., 2002. Recombinant expression and purification of an enzymatically active cysteine proteinase of the protozoan parasite *Entamoeba histolytica*. Protein Expr. Purif. 24, 131-137.

Hon C.C., Nakada-Tsukui K., Nozaki T., Guillén N., 2009. Dissecting the actin

cytoskeleton of *Entamoeba histolytica* from a genomic perspective. Anaerobic Protists Chapter 4, 81-118.

Hughes C.S., Postovit L.M., Lajoie G.A., 2010. Matrigel: a complex protein mixture required for optimal growth of cell culture. Proteomics 10, 1886-1890.

Irmer H., Tillack M., Biller L., Handal G., Leippe M., Roeder T., Tannich E., Bruchhaus I., 2009. Major cysteine peptidases of *Entamoeba histolytica* are required for aggregation and digestion of erythrocytes but are dispensable for phagocytosis and cytopathogenicity. Mol. Microbiol. 72, 658-667.

Kaushik S., Cuervo A.M., 2012. Chaperone-mediated autophagy: a unique way to enter the lysosome world. Trends Cell Biol. 22, 407-417.

Labruyère E., Guillén N., 2006. Host tissue invasion by *Entamoeba histolytica* is powered by motility and phagocytosis. Arch. Med. Res. 2006. 37, 253-258.

Leippe M., 1997. Amoebapores. Parasitol. Today 13, 178-183.

Leippe M., Bruhn H., Hecht O., Grotzinger J., 2005. Ancient weapons: the three dimensional structure of amoebapore A. Trends Parasitol. 21, 5-7.

Leroy A., Mareel M., De Bruyne G., Bailey G., Nelis H., 1995. Metastasis of *Entamoeba histolytica* compared to colon cancer: one more step in invasion. Inv. Metastasis 14, 177-191.

Liotta L.A., 1984. Tumor invasion and metastases: role of the basement membrane. Am. J. Pathol. 117, 339-348.

Loibl M., Strahl S., 2013. Protein *O*-mannosylation: what we have learned from baker's yeast. Biochim. Biophys. Acta 1833, 2438-2446.

Luzio J.P., Hackmann Y., Dieckmann N.M., Griffiths G.M., 2014. The biogenesis of lysosomes and lysosome-related organelles. Cold Spring Harb. Perspect. Biol. 2, a016840.

Luzio J.P., Parkinson M.D., Gray S.R., Bright N.A., 2009. The delivery of endocytosed cargo to lysosomes. Biochem. Soc. Trans. 37, 1019-1021.

Luzio J.P., Pryor P.R., Bright N.A., 2007. Lysosomes: fusion and function. Nat. Rev. Mol. Cell Biol. 8, 622-632.

MacFarlane R.C., Singh U., 2006. Identification of differentially expressed genes in virulent and nonvirulent *Entamoeba* species: potential implications for amebic pathogenesis. Infect. Immun. 74, 340-351.

MacFarlane R.C., Singh U., 2007. Identification of an *Entamoeba histolytica* serine-, threonine-, and isoleucine-rich protein with roles in adhesion and cytotoxicity. Eukaryot. Cell 6, 2139-2146.

Maeda Y., Kinoshita T., 2008. Dolichol-phosphoate mannose synthase: structure, function and regulation. Biochim. Biophys. Acta. 1780, 861-868.

Melendez-Lopez S.G., Herdman S., Hirata K., Choi M.H., Choe Y., Craik C., Caffrey C.R., Hansel, E., Chavez-Munguia B., Chen Y.T., Roush W.R., McKerrow J., Eckmann L., Guo J., Stanley Jr. S.L., Reed S.L., 2007. Use of recombinant *Entamoeba histolytica* cysteine proteinase 1 to identify a potent inhibitor of amebic invasion in a human colonic

model. Eukaryot. Cell 6, 1130-1136.

Meza I., Talamás-Rohana P., Vargas M.A., 2006. The cytoskeleton of *Entamoeba histolytica*: structure, function, and regulation by signaling pathways. Arch. Med. Res. 37. 234-243.

Mi-ichi F., Makiuchi T., Furukawa A., Sato D. and Nozaki T., 2011. Sulfate activation in mitosomes plays a crucial role in the proliferation of *Entamoeba histolytica*. PLoS Neglect. Trop. Dis. 5, e1263.

Mitra B.N., Saito-Nakano Y., Nakada-Tsukui K., Sato D., Nozaki T., 2007. Rab11B small GTPase regulates secretion of cysteine proteases in the enteric protozoan parasite *Entamoeba histolytica*. Cell. Microbiol. 9, 2112-2125.

Mizushima N., Levine B., Cuervo A.M., Klionsky D.J., 2008. Autophagy fights disease through cellular self-digestion. Nature 28, 1069-1075.

Moncada D., Keller K., Ankri S., Mirelman D., Chadee K., 2006. Antisense inhibition of *Entamoeba histolytica* cysteine proteases inhibits colonic mucus degradation. Gastroenterology, 130, 721-30.

Morf L., Pearson R.J., Wang A.S., Singh U., 2013. Robust gene silencing mediated by antisense small RNAs in the pathogenic protist *Entamoeba histolytica*. Nucleic Acids Res. 41, 9424-9437.

Nakada-Tsukui K., Saito-Nakano Y., Husain A., Nozaki T., 2010. Conservation and function of Rab small GTPases in *Entamoeba*: annotation of *E. invadens* Rab and its use for the understanding of *Entamoeba* biology. Exp. Parasitol. 126, 337-347.

Nakada-Tsukui K., Sekizuka T., Sato-Ebine E., Escueta-de Cadiz A., Ji D.D., Tomii K., Kuroda M., Nozaki T., 2018. AIG1 affects *in vitro* and *in vivo* virulence in clinical isolates of *Entamoeba histolytica*. PLoS Pathog. 19, e1006882.

Nakada-Tsukui K., Okada H., Mitra B.N., Nozaki T., 2009. Phosphatidylinositolphosphates mediate cytoskeletal reorganization during phagocytosis via a unique modular protein consisting of RhoGEF/DH and FYVE domains in the parasitic protozoon *Entamoeba histolytica*. Cell. Microbiol. 11, 1471-1491.

Nakada-Tsukui K., Saito-Nakano Y., Ali V., Nozaki T., 2005. A retromerlike complex is a novel Rab7 effector that is involved in the transport of the virulence factor cysteine protease in the enteric protozoan parasite *Entamoeba histolytica*. Mol. Biol. Cell 16, 5294-5303.

Nakada-Tsukui K., Tsuboi K., Furukawa A., Yamada Y., Nozaki T., 2012. A novel class of cysteine protease receptors that mediate lysosomal transport. Cell. Microbiol. 14, 1299-1317.

Nakatsu F., Ohno H., 2003. Adaptor protein complexes as the key regulators of protein sorting in the post-Golgi network. Cell Struct. Funct. 28, 419-429.

Nozaki T., Asai T., Sanchez L.B., Kobayashi S., Nakazawa M., Takeuchi T., 1999. Characterization of the gene encoding serine acetyltransferase, a regulated enzyme of cysteine biosynthesis from the protist parasites *Entamoeba histolytica* and *Entamoeba dispar*. Regulation and possible function of the cysteine biosynthetic pathway in *Entamoeba*. J. Biol.

Chem. 274, 32445-32452.

Okada M., Huston C.D., Oue M., Mann B.J., Petri Jr. W.A., Kita K., Nozaki T., 2006. Kinetics and strain variation of phagosome proteins of *Entamoeba histolytica* by proteomic analysis. Mol. Biochem. Parasitol. 145, 171-183.

Penuliar G.M., Nakada-Tsukui K., Nozaki T., 2015. Phenotypic and transcriptional profiling in *Entamoeba histolytica* reveal costs to fitness and adaptive responses associated with metronidazole resistance. Front. Microbiol. 6, 1-17.

Penuliar G.M., Furukawa A., Nakada-Tsukui K., Husain A., Sato D., Nozaki T., 2012. Transcriptional and functional analysis of trifluoromethionine resistance in *Entamoeba histolytica*. J. Antimicrob. Chemother. 67, 375-386.

Petri Jr. W.A., Haque R., Mann B.J., 2002. The bittersweet interface of parasite and host: lectin-carbohydrate interactions during human invasion by the parasite *Entamoeba histolytica*. Annu. Rev. Microbiol. 56, 39-64.

Petrie R.J., Gavara N., Chadwick R.S., Yamada K.M., 2012. Nonpolarized signaling reveals two distinct modes of 3D cell migration. J. Cell Biol. 30, 439-55.

Petrie R.J., Yamada K.M., 2016. Multiple mechanisms of 3D migration: the origins of plasticity. Curr. Opin. Cell Biol. 42, 7-12.

Polishchuk E.V., Polishchuk R.S., 2016. The emerging role of lysosomes in copper homeostasis. Metallomics 8, 853-862.

Punta M., Coggill P.C., Eberhardt R.Y., Mistry J., Tate J., Boursnell C., Pang N., Forslund

K., Ceric G., Clements J., Heger A., Holm L., Sonnhammer E.L., Eddy S.R., Bateman A., Finn R.D., 2012. The Pfam protein families database. Nucl. Acids Res. 40 (Database issue), D290–D301.

Purchio A.F., Cooper J.A., Brunner A.M., Lioubin M.N., Gentry L.E., Kovacina K.S., Roth R.A., Marquardt H., 1988. Identification of mannose 6-phosphate in two asparagine-linked sugar chains of recombinant transforming growth factor-β1 precursor. J. Biol. Chem. 5, 14211-14215.

Que X., Kim S.H., Sajid M., Eckmann L., Dinarello C.A., McKerrow J.H., Reed S.L., 2003. A surface amebic cysteine proteinase inactivates interleukin-18. Infect. Immun. 71, 1274-1280.

Que X., Reed S.L., 2000. Cysteine proteinases and the pathogenesis of amebiasis. Clin. Microbiol. Rev. 13, 196-206.

Ralston K.S., Petri Jr. W.A., 2011. Tissue destruction and invasion by *Entamoeba histolytica*. Trends Parasitol. 27, 254-263.

Ravdin J.I., Guerrant R.L., 1981. Role of adherence in cytopathogenic mechanisms of *Entamoeba histolytica*. Study with mammalian tissue culture cells and human erythrocytes. J. Clin. Invest. 68, 1305-1313.

Ravdin J.I., Stanley P., Murphy C.F., Petri Jr. W.A.,1989. Characterization of cell surface carbohydrate receptors for *Entamoeba histolytica* adherence lectin. Infect. Immun. 57, 2179-2186.

Riekenberg S., Flockenhaus B., Vahrmann A., Muller M.C., Leippe M., Kiess M., Scholze H., 2004. The β-N-acetylhexosaminidase of *Entamoeba histolytica* is composed of two homologous chains and has been localized to cytoplasmic granules. Mol. Biochem. Parasitol. 138, 217-225.

Saftig P., Klumperman J., 2009. Lysosome biogenesis and lysosomal membrane proteins: trafficking meets function. Nat. Rev. Mol. Cell Biol. 10, 623-635.

Sambrook J., Russell D.W., 2001. Molecular Cloning. Cold Spring Harbor Laboratory Press, New York.

Schmidt A., Hall M.N., 1998. Signaling to the actin cytoskeleton. Annu. Rev. Cell Dev. Biol. 14, 305-338.

Settembre C., Fraldi A., Medina D.L., Ballabio A., 2013. Signals from the lysosome: a control centre for cellular clearance and energy metabolism. Nat. Rev. Mol. Cell Biol. 14, 283-296.

Shah M., Foreman D.M., Ferguson M.W., 1992. Control of scarring in adult wounds by neutralising antibody to transforming growth factor β. Lancet. 25, 213-214.

Shah M., Foreman D.M., Ferguson M.W., 1994. Neutralising antibody to TGF-β 1,2 reduces cutaneous scarring in adult rodents. J. Cell Sci. 107, 1137-1157.

Stanley S.L. Jr., 2003. Amoebiasis. Lancet. 22, 1025-34.

Staudt C., Puissant E., Boonen M., 2016. Subcellular trafficking of mammalian lysosomal proteins: an extended view. Int. J. Mol. Sci. 18, pii: E47.

Steven F.S., 1964. The nishihara technique for the solubilization of collagen: Application to the preparation of soluble collagens from normal and rheumatoid connective tissue. Ann. Rheum. Dis. 23, 300-301.

Stewart-Tull D.E., Ollar R.A., Scobie T.S., 1986. Studies on the *Vibrio cholerae* mucinase complex. I. Enzymic activities associated with the complex. J. Med. Microbiol. 22, 325-333.

Tavares P., Sansonetti P., Guillén N., 2000. Cell polarization and adhesion in a motile pathogenic protozoan: role and fate of the *Entamoeba histolytica* Gal/GalNAc lectin. Microbes Infect. 2, 643-649.

Thibeaux R., Ave P., Bernier M., Morcelet M., Frileux P., Guillén N., Labruyere E., 2014. The parasite *Entamoeba histolytica* exploits the activities of human matrix metalloproteinases to invade colonic tissue. Nat. Commun. 5, 5142.

Thibeaux R., Weber C., Hon C.C., Dillies M.A., Ave P., Coppee J.Y., Labruyere E., Guillén N., 2013. Identification of the virulence landscape essential for *Entamoeba histolytica* invasion of the human colon. PLoS Pathog. 9, e1003824.

Tillack M., Biller L., Irmer H., Freitas M., Gomes M.A., Tannich E., Bruchhaus I., 2007. The *Entamoeba histolytica* genome: primary structure and expression of proteolytic enzymes. BMC Genomics 8, 170.

Whyte J.R., Munro S., 2001. A yeast homolog of the mammalian mannose 6-phosphate receptors contributes to the sorting of vacuolar hydrolases. Curr. Biol. 11, 1074-1078.

Ximénez C., Morán P., Rojas L., Valadez A., Gómez A., 2009. Reassessment of the epidemiology of amebiasis: state of the art. Infect. Genet. Evol. 9, 1023-1032.

Yeats C., Bentley S., Bateman A., 2003. New knowledge from old: *in silico* discovery of novel protein domains in *Streptomyces coelicolor*. BMC Microbiol. 3, 3.

Yousuf M.A., Mi-ichi F., Nakada-Tsukui K., Nozaki T., 2010. Localization and targeting of an unusual pyridine nucleotide transhydrogenase in *Entamoeba histolytica*. Eukaryot. Cell 9, 926-933.

TABLES

Table 1. LC-MS/MS data of 70 kDa cysteine protease binding protein family 2 (CPBF2)-interacting protein.

No.	Identified proteins	GenBank gi number	Molecular weight	Total specrum count
1	α-amylase family protein (*Entamoeba histolytica* HM-1:IMSS)	gi|67480699	69 kDa	16
2	hypothetical protein (*Entamoeba histolytica* HM-1:IMSS)	gi|183230151	48 kDa	1

Table 2. Ligands and associated proteins of cysteine protease binding protein family (CPBF) 2-11 identified by immunoprecipitation and LC-MS/MS analysis.

CPBF	Identified proteins	Molecular weight	Accession number		Quantitative value[d]		Unique peptides[e]	
			GenBank	AmoebaDB	CPBF	HA	CPBF	HA
					CPBF2		CPBF2	
CPBF2	CPBF2	97 kDa	XP_653276	EHI_087660	348.17	0	43	0
	α-Amylase family protein	69 kDa	XP_655699	EHI_152880	122.46	0	25	0
	70 kDa heat shock protein	73 kDa	XP_654737	EHI_199590	3.37	0	3	0
	Hypothetical protein	24 kDa	XP_655760	EHI_155310	3.37	0	1	0
					CPBF3			
CPBF3	CPBF3	96 kDa	XP_649180	EHI_161650	203.48	0	42	0
	70 kDa heat shock protein	73 kDa	XP_654737	EHI_199590	14.8	2.64	12	3
	CPBF4	98 kDa	XP_655897	EHI_012340	12.02	0	1	0
					CPBF4			
CPBF4	CPBF4	98 kDa	XP_655897	EHI_012340	152.3	0	34	0
	CPBF3	96 kDa	XP_649180	EHI_161650	15.49	0	2	0
	Serine-therionine-isoleucine rich protein	260 kDa	XP_001913596	EHI_004340	4.3	0	4	0
	EhCP-A2	35 kDa	XP_650642	EHI_033710	3.44	0	3	0
	Galactose-specific lectin light subunit	34 kDa	XP_001913429	EHI_049690	3.44	0	4[f]	0
					CPBF5			
CPBF5	CPBF5	96 kDa	XP_654065	EHI_137940	172.19	0	33	0
	70 kDa heat shock protein	73 kDa	XP_654737	EHI_199590	12.98	0	7	0
	Galactose-specific lectin light subunit	34 kDa	XP_656145	EHI_035690	6.92	0	5	0
	Hypothetical protein	34 kDa	XP_650601	EHI_047800	3.46	0	3	0
CPBF6[a]	CPBF6	99 kDa	XP_653036	EHI_178470				
	α-Amylase family protein	57 kDa	XP_655636	EHI_023360				
	γ-Amylase	75 kDa	XP_652381	EHI_044370				
					CPBF7			
CPBF7	CPBF7	100 kDa	XP_649361	EHI_040440	344.3	3.14	33	0
	β-N-acetylhexosaminidase	64 kDa	XP_656208	EHI_012010	17.95	0	5	0
	β-N-acetylhexosaminidase, subunit	64 kDa	XP_650273	EHI_007330	16.32	0	5	0
	MPR1	24 kDa	XP_656907	EHI_096320	13.06	0	4	0
	Pore-forming peptide amoebapore B precursor	10 kDa	XP_001913632	EHI_194540	9.79	0	3	0
	70 kDa heat shock protein	73 kDa	XP_654737	EHI_199590	8.16	0	4	0
	Hypothetical protein	30 kDa	XP_652382	EHI_044360	6.53	3.14	2	1
	Hypothetical protein	17 kDa	XP_650886	EHI_069510	3.26	1.57	1	1
	Hypothetical protein	24 kDa	XP_655760	EHI_155310	3.26	0	1	0
	Hypothetical protein	59 kDa	XP_656261	EHI_178650	3.26	0	2	0
CPBF8[b]	CPBF8	100 kDa	XP_652899	EHI_059830				
	β-hexosaminidase, "alpha" sign-subunit	60 kDa	XP_65729/AJ582954[c]	EHI_148130				
	Lysozyme1	23 kDa	XP_653294	EHI_199110				
	Lysozyme2	23 kDa	XP_656933	EHI_096570				
					CPBF9			
CPBF9	CPBF9	100 kDa	XP_655360	EHI_021220	100.27	0	18	0
	Hypothetical protein	18 kDa	XP_656071	EHI_117850	10.29	0	1	0
	70 kDa heat shock protein	73 kDa	XP_654737	EHI_199590	10.29	0	3	0
	Lysozyme2	23 kDa	XP_656933	EHI_096570	7.71	1.52	1	1
					CPBF10			
CPBF10	CPBF10	98 kDa	XP_649015	EHI_191730	63.88	0	12	0
	α-Amylase	53 kDa	XP_656406	EHI_153100	49.05	0	10	0
	α-Amylase family protein	57 kDa	XP_655636	EHI_023360	27.38	5.76	10	4
	70 kDa heat shock protein	73 kDa	XP_654737	EHI_199590	25.09	4.61	11	3
	Hypothetical protein	59 kDa	XP_656261	EHI_178650	19.39	0	6	0
	β-Amylase	47 kDa	XP_653896	EHI_192590	17.11	2.31	6	2
	Hypothetical protein	71 kDa	XP_651525	EHI_022130	4.56	0	3	0
	Hypothetical protein	57 kDa	XP_648234	EHI_025100	4.56	0	3	0
	MPR1	24 kDa	XP_656907	EHI_096320	3.42	0	3	0
					CPBF11			
CPBF11	CPBF11	86 kDa	XP_656044	EHI_118120	89.53	0	23	0
	70 kDa heat shock protein	73 kDa	XP_654737	EHI_199590	24.11	4.61	17	3

HA, hemagglutinin; EhCP, *Entamoeba histolytica* cysteine protease; MPR, mannose 6-phosphate receptor

[a] From Furukawa *et al*. (2013).

[b] From Furukawa *et al*. (2012)

[c] XP_657529 (EHI_148130) and AJ582954 are identical except that XP_65729 (EHI_148130) starts at the second methionine of AJ582954 and lacks the signal sequence.

[d] Quantitative values are shown for the identified proteins from the CPBF-HA and control transformants.

[e] The number of unique peptides detected are shown.

[f] This protein is similar to two other closely related proteins and the number of all detected peptides is shown.

Table 3. LC-MS/MS data of 60, 55 and 40 kDa cysteine protease binding protein family 10 (CPBF10)-interacting protein.

No.	Identified proteins	GenBank gi number	Molecular weight	Total specrum count
60 kDa band				
1	α-amylase family protein (*Entamoeba histolytica* HM-1:IMSS)	gi|183230432	57 kDa	24
2	α-amylase (*Entamoeba histolytica* HM-1:IMSS)	gi|67482113	53 kDa	20
3	malic enzyme (*Entamoeba histolytica* HM-1:IMSS)	gi|67464797	53 kDa	5
4	α-amylase (*Entamoeba histolytica* HM-1:IMSS)	gi|67471047	50 kDa	4
5	ATP/GTP-binding protein (*Entamoeba histolytica* HM-1:IMSS)	gi|67477909	48 kDa	1
6	hypothetical protein (*Entamoeba histolytica* HM-1:IMSS)	gi|67469553	26 kDa	1
55kDa band				
1	α-amylase (*Entamoeba histolytica* HM-1:IMSS)	gi|67482113	53 kDa	31
2	α-amylase (*Entamoeba histolytica* HM-1:IMSS)	gi|67471047	50 kDa	8
3	enolase (*Entamoeba histolytica* HM-1:IMSS)	gi|67466006	47 kDa	8
4	guanine nucleotide exchange factor *(Entamoeba histolytica* HM-1:IMSS)	gi|67464925	51 kDa	6
5	Actin-related protein 3 (*Entamoeba histolytica* HM-1:IMSS)	gi|67462416	47 kDa	6
6	α-amylase family protein (*Entamoeba histolytica* HM-1:IMSS)	gi|183230432	57 kDa	4
7	alcohol dehydrogenase (*Entamoeba histolytica* HM-1:IMSS)	gi|183234048	47 kDa	4
8	helicase (*Entamoeba histolytica* HM-1:IMSS)	gi|67480889	47 kDa	4
9	elongation factor 1-α 1 (*Entamoeba histolytica* HM-1:IMSS)	gi|67463408	48 kDa	3
10	hypothetical protein (*Entamoeba histolytica* HM-1:IMSS)	gi|67469661	59 kDa	2
11	hypothetical protein (*Entamoeba histolytica* HM-1:IMSS)	gi|67477467	23 kDa	1
12	anti-*Entamoeba histolytica* immunoglobulin γ heavy chain (Homo sapiens)	gi|5360677	24 kDa	1
13	actin (*Entamoeba histolytica* HM-1:IMSS)	gi|67462785	42 kDa	1
14	hypothetical protein (*Entamoeba histolytica* HM-1:IMSS)	gi|183235174	150 kDa	1
15	DNA primase small subunit (*Entamoeba histolytica* HM-1:IMSS)	gi|183235176	22 kDa	1
16	phosphoglycerate kinase (*Entamoeba histolytica* HM-1:IMSS)	gi|67476166	45 kDa	1
17	hypothetical protein (*Entamoeba histolytica* HM-1:IMSS)	gi|67472989	37 kDa	1
18	acid phosphatase (*Entamoeba histolytica* HM-1:IMSS)	gi|67467196	49 kDa	1
19	hypothetical protein (*Entamoeba histolytica* HM-1:IMSS)	gi|183230572	47 kDa	1
20	elongation factor 1-alpha 1 (*Entamoeba histolytica* HM-1:IMSS)	gi|67471927	48 kDa	1
21	hypothetical protein (*Entamoeba histolytica* HM-1:IMSS)	gi|67481643	82 kDa	1
40 kDa band				
1	alcohol dehydrogenase (*Entamoeba histolytica* HM-1:IMSS)	gi|67479581	43 kDa	4
2	α-amylase *(Entamoeba histolytica* HM-1:IMSS)	gi|67482113	53 kDa	3
3	enhancer binding protein-1 (*Entamoeba histolytica* HM-1:IMSS)	gi|67471742	35 kDa	2
4	hypothetical protein (*Entamoeba histolytica* HM-1:IMSS)	gi|67476757	38 kDa	2
5	NADP-dependent alcohol dehydrogenase (*Entamoeba histolytica* HM-1:IMSS)	gi|67475633	39 kDa	2
6	actin (*Entamoeba histolytica* HM-1:IMSS)	gi|67462785	42 kDa	1
7	hypothetical protein (*Entamoeba histolytica* HM-1:IMSS)	gi|183235174	150 kDa	1
8	hypothetical protein (*Entamoeba histolytica* HM-1:IMSS)	gi|67477467	23 kDa	1
9	hypothetical protein (*Entamoeba histolytica* HM-1:IMSS)	gi|67478285	151 kDa	1
10	hypothetical protein (*Entamoeba histolytica* HM-1:IMSS)	gi|67483075	29 kDa	1
11	hypothetical protein (*Entamoeba histolytica* HM-1:IMSS)	gi|67483069	57 kDa	1
12	actin-related protein 2/3 complex subunit 1A (*Entamoeba histolytica* HM-1:IMSS)	gi|67484080	40 kDa	1
13	alcohol dehydrogenase (*Entamoeba histolytica* HM-1:IMSS)	gi|67468848	42 kDa	1
14	helicase *(Entamoeba histolytica* HM-1:IMSS)	gi|183233848	110 kDa	1
15	malate dehydrogenase *(Entamoeba histolytica* HM-1:IMSS)	gi|183232436	40 kDa	1
16	leukocyte-endothelial cell adhesion molecule 3 (*Entamoeba histolytica* HM-1:IMSS)	gi|67467899	36 kDa	1
17	alcohol dehydrogenase (*Entamoeba histolytica* HM-1:IMSS)	gi|67476643	43 kDa	1
18	L-asparaginase (*Entamoeba histolytica* HM-1:IMSS)	gi|67482473	41 kDa	1
19	TolA-like protein (*Entamoeba histolytica* HM-1:IMSS)	gi|67471361	38 kDa	1
20	AIG1 family protein (*Entamoeba histolytica* HM-1:IMSS)	gi|183237430	33 kDa	1
21	Sec61 α subunit (*Entamoeba histolytica*)	gi|52352493	52 kDa	1

Table 4. Reproducibility of identified cysteine protease binding protein family 1 (CPBF1) binding proteins.

Identified proteins	Molecular weight	Accession number		Number of experiments in which the protein was identified
		GenBank gi number	AmoebaDB	
CPBF1	101 kDa	XP_655218	EHI_164800	4
EhCP-A2	35 kDa	XP_650642	EHI_033710	4
EhCP-A4	34 kDa	XP_656602	EHI_050570	4
EhCP-A5	35 kDa	XP_650937	EHI_168240	4
70kDa heat shock protein	73 kDa	XP_654737	EHI_199590	3
Mannosyltransferase	49 kDa	XP_650080	EHI_029580	2
Hypothetical protein	43 kDa	XP_649888	EHI_146110	2

EhCP, *Entamoeba histolytica* cysteine protease.

Table 5. Ligands and associated proteins of cysteine protease binding protein family 1 (CPBF1) identified in four independent experiments.

Exp. ID	Identified proteins	Molecular weight	Accession number		Quantitative value	
			GenBank	AmoebaDB	CPBF1	HA
1787-1	CPBF1	101 kDa	XP_655218.1	EHI_164800	471.75	8.97
	EhCP-A5	35 kDa	XP_650937.1	EHI_168240	76.26	0.00
	PIG-X domain	58 kDa	XP_648739.1	EHI_130880	38.77	0.00
	EhCP-A2	35 kDa	XP_650642.1	EHI_033710	28.43	0.00
	EhCP-A4	34 kDa	XP_656602.1	EHI_050570	25.85	0.00
	nuclear poar protein	186 kDa	XP_654325.1	EHI_183510	19.39	3.26
	EhCP-A1	35 kDa	XP_650156.2	EHI_074180	12.92	0.00
	EhCP-A6	35 kDa	XP_657364.1	EHI_151440	9.05	0.00
	DNAJ homolog subfamily A member 1	39 kDa	XP_656707.2	EHI_182520	6.46	0.00
	mannosyltransferase	49 kDa	XP_650080.1	EHI_029580	6.46	0.00
	MIR domain protein	23 kDa	XP_655109.1	EHI_100480	6.46	0.00
	protein disulfide isomerase	42 kDa	XP_650651.1	EHI_071590	3.88	0.82
1814b	CPBF1	101 kDa	XP_655218.1	EHI_164800	70.41	1.57
	hypothetical protein	71 kDa	XP_651525.1	EHI_022130	8.06	1.57
	galactose-inhibitable lectin 35 kda subunit precursor	34 kDa	XP_656145.1	EHI_035690	6.45	1.57
	70 kDa heat shock protein	73 kDa	XP_654737.1	EHI_199590	6.45	0.00
	EhCP-A4	34 kDa	XP_656602.1	EHI_050570	5.37	0.00
	Gal/GalNAc lectin light subunit	32 kDa	XP_657460.1	EHI_148790	4.30	0.00
	EhCP-A5	35 kDa	XP_650937.1	EHI_168240	3.76	1.57
	hypothetical protein	43 kDa	XP_649888.1	EHI_146110	3.22	1.57
1830A	CPBF1	101 kDa	XP_655218.1	EHI_164800	219.14	0.00
	hypothetical protein	34 kDa	XP_649236.1	EHI_160980	13.91	3.81
	70 kDa heat shock protein, putative	73 kDa	XP_654737.1	EHI_199590	10.44	0.00
	EhCP-A5	35 kDa	XP_650937.1	EHI_168240	9.28	0.00
	hypothetical protein	43 kDa	XP_649888.1	EHI_146110	6.96	2.28
	hypothetical protein	55 kDa	XP_649879.1	EHI_001100	6.96	0.00
	EhCP-A4	34 kDa	XP_656602.1	EHI_050570	6.96	0.00
	CPBF3	96 kDa	XP_649180.2	EHI_161650	5.80	0.76
	EhCP-A2	35 kDa	XP_650642.1	EHI_033710	5.80	0.00
1875	CPBF1	101 kDa	XP_655218.1	EHI_164800	260.13	0.88
	EhCP-A5	35 kDa	XP_650937.1	EHI_168240	22.62	0.00
	70 kDa heat shock protein, putative	73 kDa	XP_654737.1	EHI_199590	22.62	2.64
	EhCP-A2	35 kDa	XP_650642.1	EHI_033710	9.69	0.00
	EhCP-A4	34 kDa	XP_656602.1	EHI_050570	8.08	0.00
	mannosyltransferase, putative	49 kDa	XP_650080.1	EHI_029580	3.23	0.00

EhCP, *Entamoeba histolytica* cysteine protease; MIR, [Mannosyltransferase,
Inositol 1,4,5-trisphosphate receptor (IP3R); Ryanodine receptor (RyR)]; HA, hemagglutinin.
Experiment identification numbers (Exp. ID), used in MS analysis at Biomedical Mass Spectrometry Laboratory, University of Virginia, USA are shown.

Table 6. Percentage of mutual identity among cysteine protease binding protein families (CPBFs).

	CPBF1	CPBF2	CPBF3	CPBF4	CPBF5	CPBF6	CPBF7	CPBF8	CPBF9	CPBF10	CPBF11
CPBF1	100	25.6	23.9	24.9	25	22.4	20.1	20.2	23.8	20	21.6
CPBF2		100	24.1	23.1	30.1	21.8	21.1	20.2	25.5	20.5	18.7
CPBF3			100	74.8	22.1	22.8	21.7	22.6	20.4	20.4	29.1
CPBF4				100	20.2	22.2	20.8	21.7	19.6	20.7	30.5
CPBF5					100	18	19.2	19.2	24.9	18.6	19.5
CPBF6						100	27.3	28.2	19.7	24.6	20
CPBF7							100	51.1	20.1	27.5	20.2
CPBF8								100	18.9	27.8	17.6
CPBF9									100	19.5	18.8
CPBF10										100	18
CPBF11											100

100~75%
75~50%
50~25%
25~10%
10~0%

Table 7. LC-MS/MS data of 45 kDa cysteine protein binding protein family 11 (CPBF11)-interacting protein.

No.	Identified proteins	GenBank gi number	Molecular weight	Total spectrum count
1	hypothetical protein (*Entamoeba histolytica* HM-1:IMSS)	gi|67481389	86 kDa	32
2	heat shock protein 90 (*Entamoeba histolytica* HM-1:IMSS)	gi|67474857	83 kDa	4
3	4-α-glucanotransferase (*Entamoeba histolytica* HM-1:IMSS)	gi|67479419	97 kDa	4
4	hypothetical protein (*Entamoeba histolytica* HM-1:IMSS)	gi|67483069	57 kDa	2
5	protein kinase domain containing protein (*Entamoeba histolytica* HM-1:IMSS)	gi|183235054	67 kDa	2
6	hypothetical protein (*Entamoeba histolytica* HM-1:IMSS)	gi|67477467	23 kDa	1
7	alcohol dehydrogenase (*Entamoeba histolytica* HM-1:IMSS)	gi|67473032	96 kDa	1
8	hypothetical protein (*Entamoeba histolytica* HM-1:IMSS)	gi|183231355	79 kDa	1
9	diaphanous protein (*Entamoeba histolytica*)	gi|7159336	122 kDa	1
10	actinin-like protein (*Entamoeba histolytica*)	gi|6636336	63 kDa	1
11	Rab GTPase activating protein (*Entamoeba histolytica* HM-1:IMSS)	gi|67467287	73 kDa	1
12	adaptor protein (AP) family protein (*Entamoeba histolytica* HM-1:IMSS)	gi|67466287	81 kDa	1
13	WD domain containing protein (*Entamoeba histolytica* HM-1:IMSS)	gi|67473313	111 kDa	1
14	ribonuclease P protein subunit p30 (*Entamoeba histolytica* HM-1:IMSS)	gi|67470047	27 kDa	1
15	Rab family GTPase (*Entamoeba histolytica* HM-1:IMSS)	gi|67481151	23 kDa	1
16	serine palmitoyltransferase (*Entamoeba histolytica* HM-1:IMSS)	gi|67483423	98 kDa	1

Table 8. Up-regulated genes in *cpbf2* -silenced strain

gene ID	Description	fold change (log2)	q_value
protein synthesis			
EHI_069310	serine palmitoyltransferase putative	2.13	3.03E-03
membrane traffic			
EHI_192130	Rab family GTPase (Rab7F)	4.05	1.48E-02
protein degradation			
EHI_169350	nonpathogenic pore-forming peptide precursor putative	4.39	3.03E-03
AIG family			
EHI_144270	AIG1 family protein	2.74	3.03E-03
EHI_176580	AIG1 family protein putative	3.79	3.03E-03
EHI_176590	AIG1 family protein putative	4.31	3.03E-03
EHI_176700	AIG1 family protein putative	4.21	3.03E-03
other			
EHI_C00154	Single TM Domain protein	4.92	3.03E-03
EHI_C00062	Two TM Domain protein	5.84	3.03E-03

FIGURES

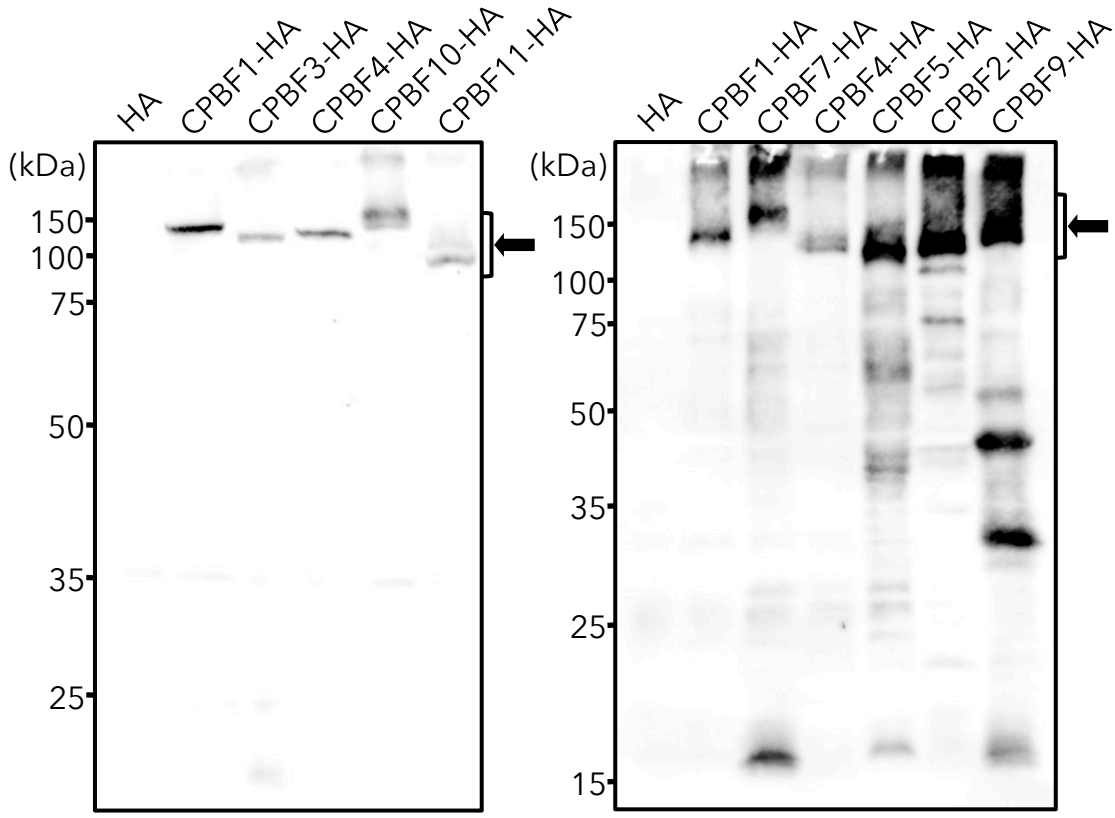

Figure 1. Immunoblot analysis to confirm the cysteine protease binding protein family 1–11 tagged with hemagglutinin (CPBF1-11-HA) expression in the *Entamoeba histolytica* transformants.

Whole lysates of the transformants were subjected to SDS-PAGE and immunoblot analysis using anti-HA antibody. Arrows indicate the individual CPBF1-11. Note that the predicted molecular mass of the fusion proteins are: CPBF1-HA, 100.7 kDa; CPBF2-HA, 96.7 kDa; CPBF3-HA, 99.1 kDa; CPBF4-HA, 99.3 kDa; CPBF5-HA, 96.5 kDa; CPBF7-HA, 100.0 kDa; CPBF9-HA, 100.0 kDa; CPBF10-HA, 97.8 kDa; CPBF11-HA, 86.3 kDa.

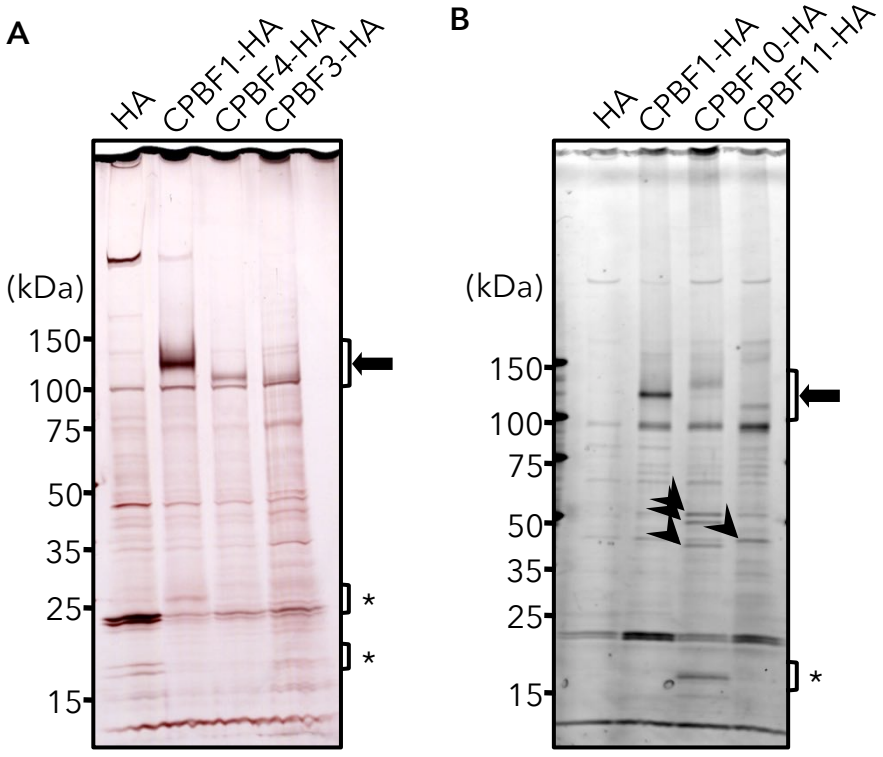
A
HA
CPBF1-HA
CPBF4-HA
CPBF3-HA
(kDa)
150
100
75
50
35
25
15
*
*
B
HA
CPBF1-HA
CPBF10-HA
CPBF11-HA
(kDa)
150
100
75
50
35
25
15
*

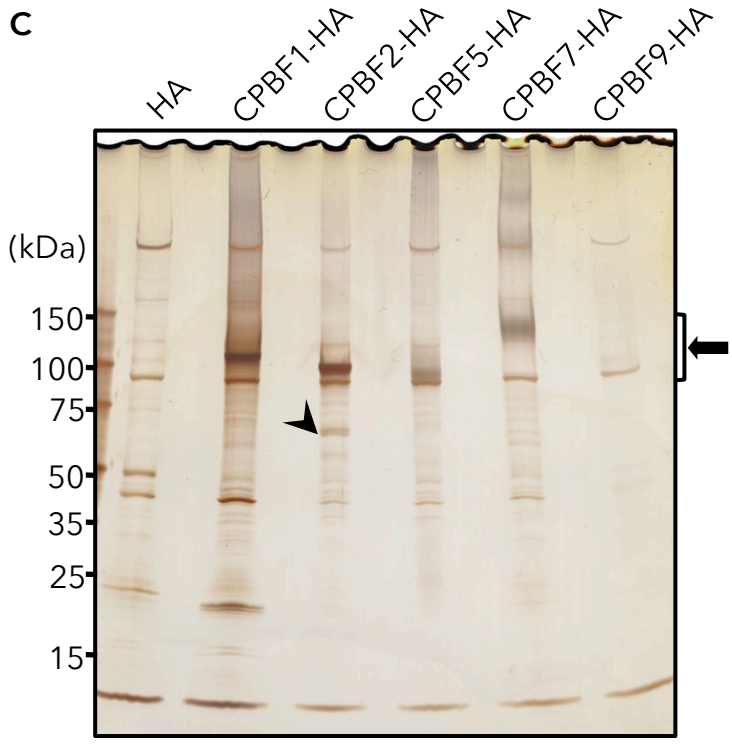

Figure 2. SDS–PAGE analysis of immunoprecipitated mixtures of *Entamoeba histolytica* cysteine protease binding protein families (CPBFs) and ligands.

CPBF1, 2, 3, 4, 5, 7, 9, 10 and 11-haemagglutinin (HA) were immunoprecipitated from the corresponding transformant lines with anti-HA monoclonal antibody, separated by SDS–PAGE and stained by (A, C) silver staining or (B) Sypro Ruby staining. (A) CPBF1, 3 and 4-HA; (B) CPBF1, 10 and 11-HA; (C) CPBF1, 2, 5, 7 and 9-HA. Arrows indicate the bait (CPBF–HA) immunoprecipitated, and arrowheads depict candidates for co-immunoprecipitated ligands. Note that immunoprecipitation and electrophoresis were conducted in three independent experiments.
* These bands were not reproducible.

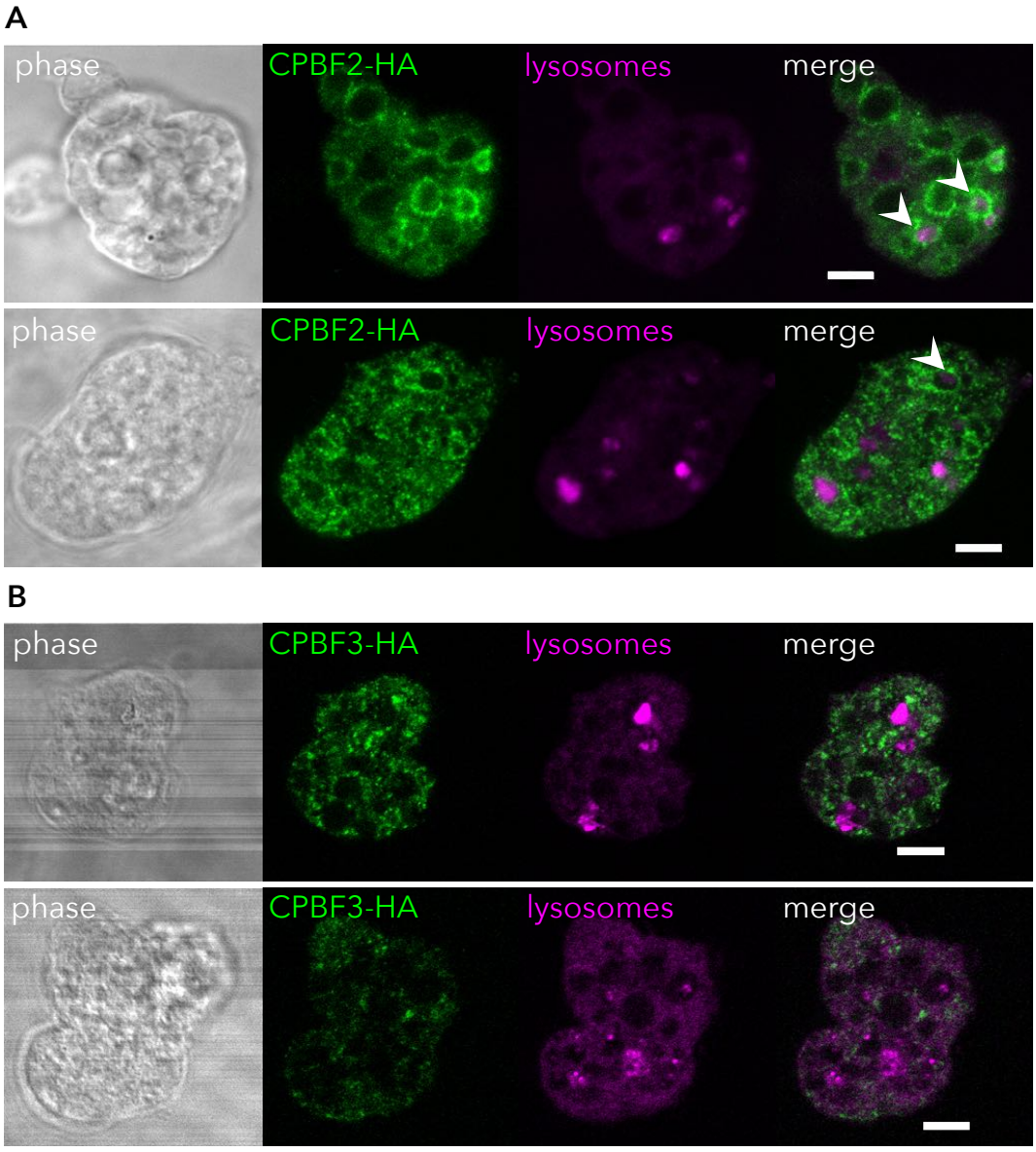
A
phase
CPBF2-HA
lysosomes
merge
phase
CPBF2-HA
lysosomes
merge
B
phase
CPBF3-HA
lysosomes
merge
phase
CPBF3-HA
lysosomes
merge

C

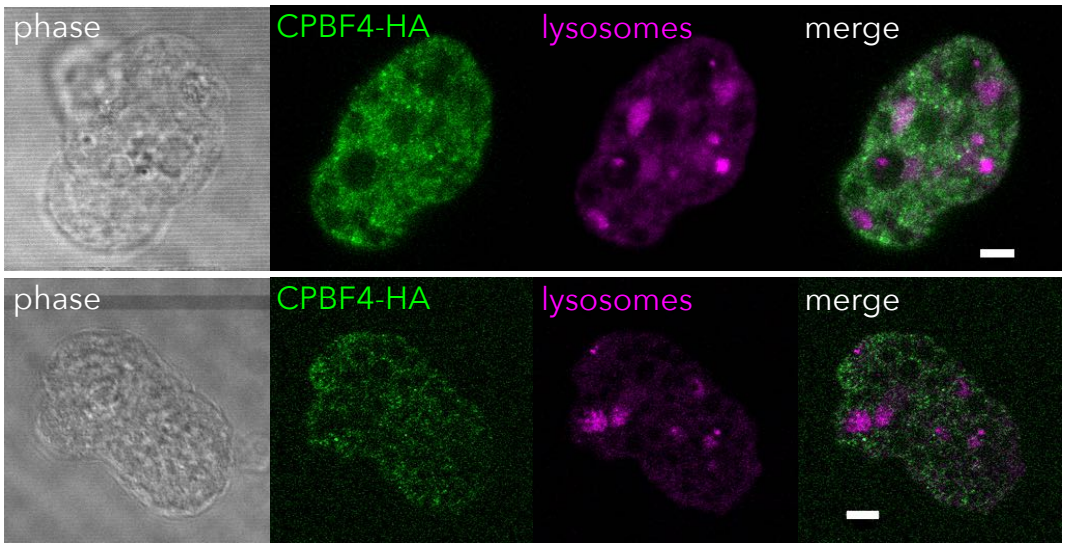
phase
CPBF4-HA
lysosomes
merge
phase
CPBF4-HA
lysosomes
merge

D

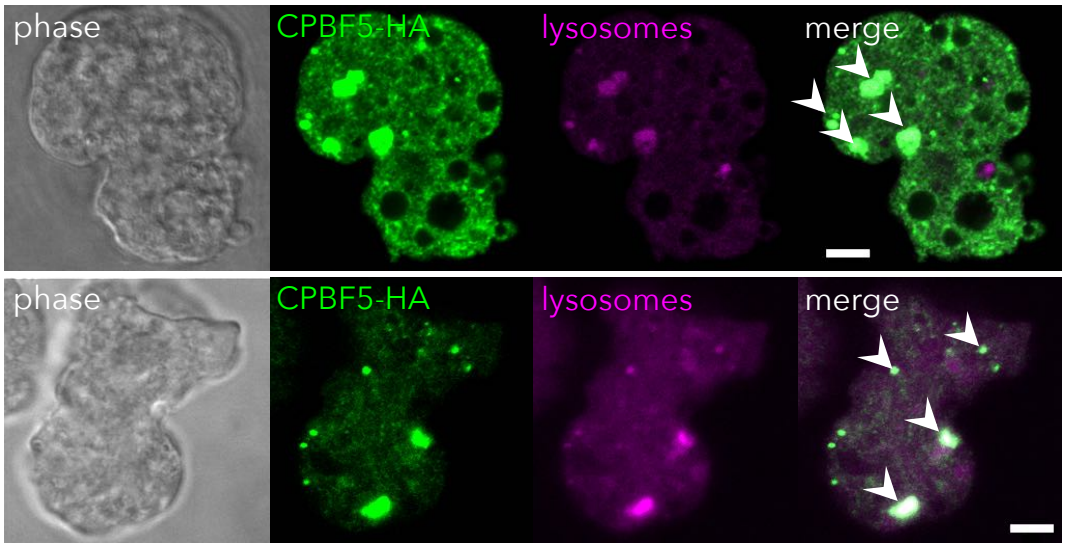
phase
CPBF5-HA
lysosomes
merge
phase
CPBF5-HA
lysosomes
merge

E

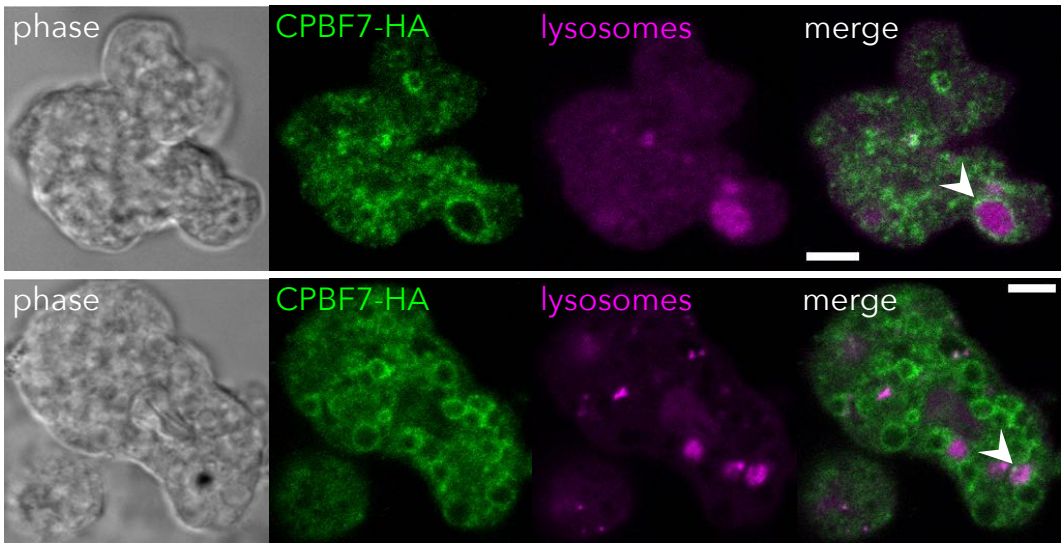
phase
CPBF7-HA
lysosomes
merge
phase
CPBF7-HA
lysosomes
merge

F

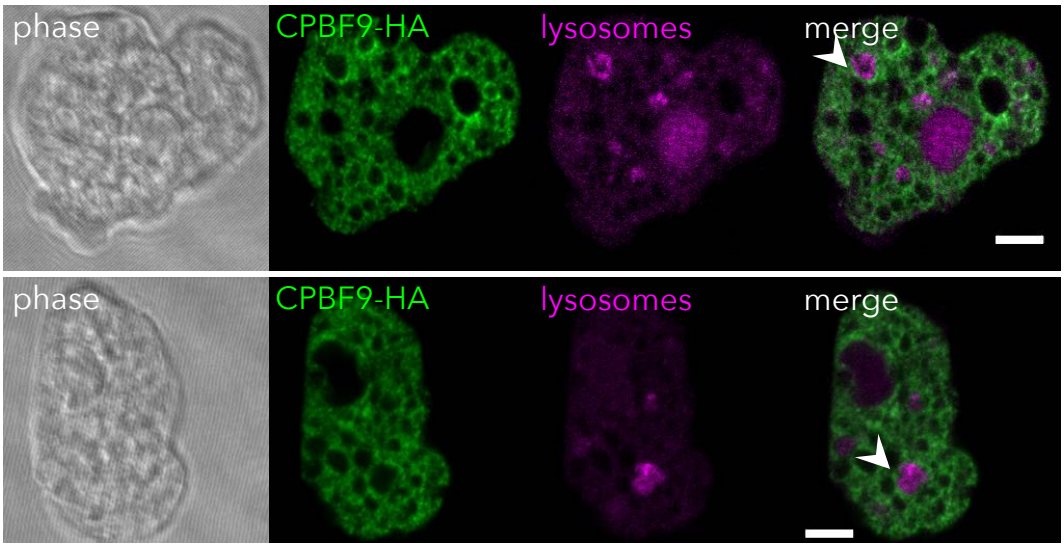
phase
CPBF9-HA
lysosomes
merge
phase
CPBF9-HA
lysosomes
merge

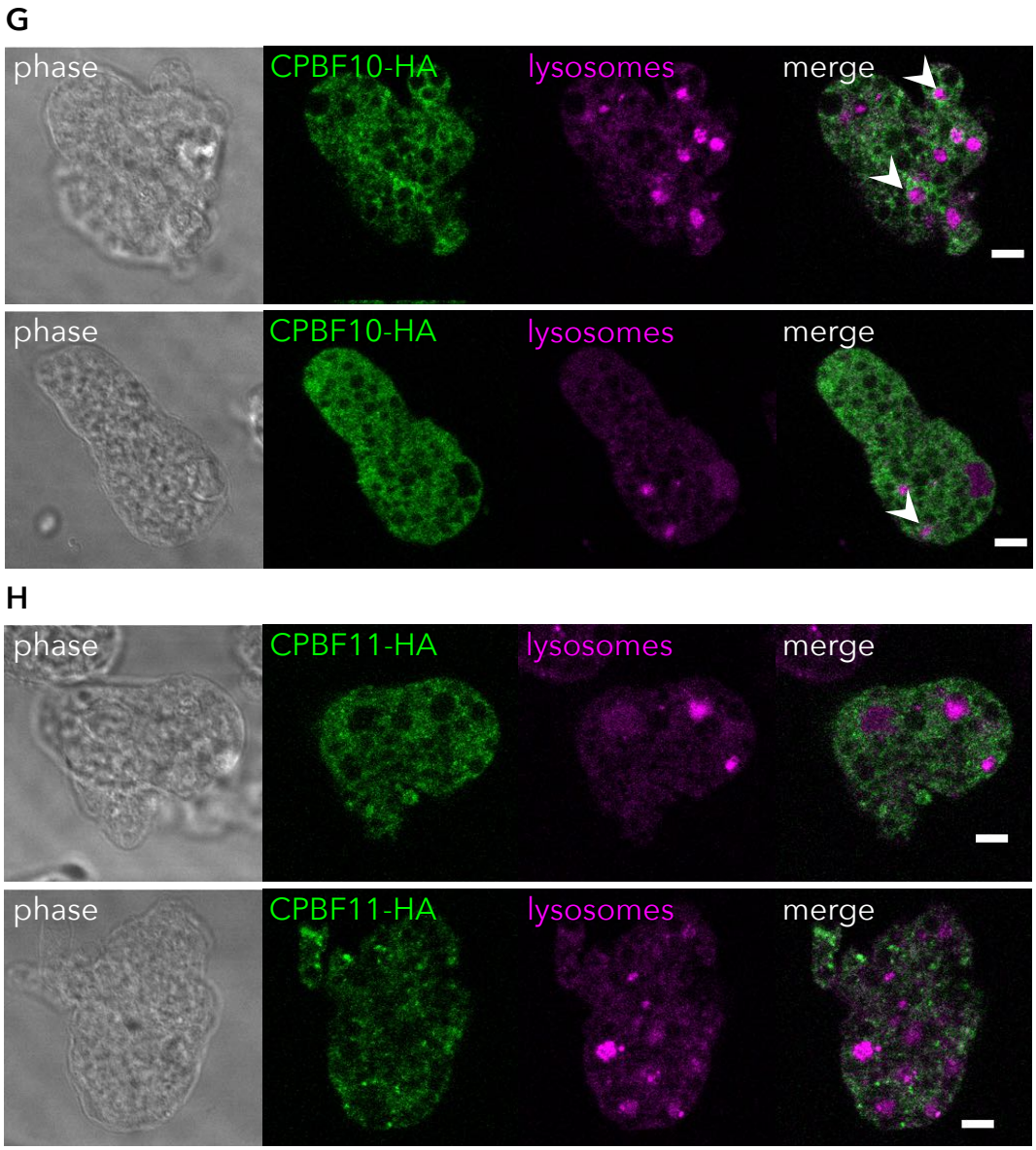

Figure 3. Immunofluorescence images of *Entamoeba histolytica* cysteine protease binding protein families (CPBFs) 2, 3, 4, 5, 7, 9, 10 and 11.

Trophozoites of the CPBF- haemagglutinin (HA)-expressing transformants were incubated with LysoTracker Red, fixed, reacted with anti-HA antibody and confocal images were captured on LSM510. Thirteen to 61 cells were examined in one to five independent experiments for each CPBF. Two representative cells are shown for each CPBF. Arrows heads depict LysoTracker accumulation in the CPBF-positive vesicles and vacuoles. Bars = 10 μm.

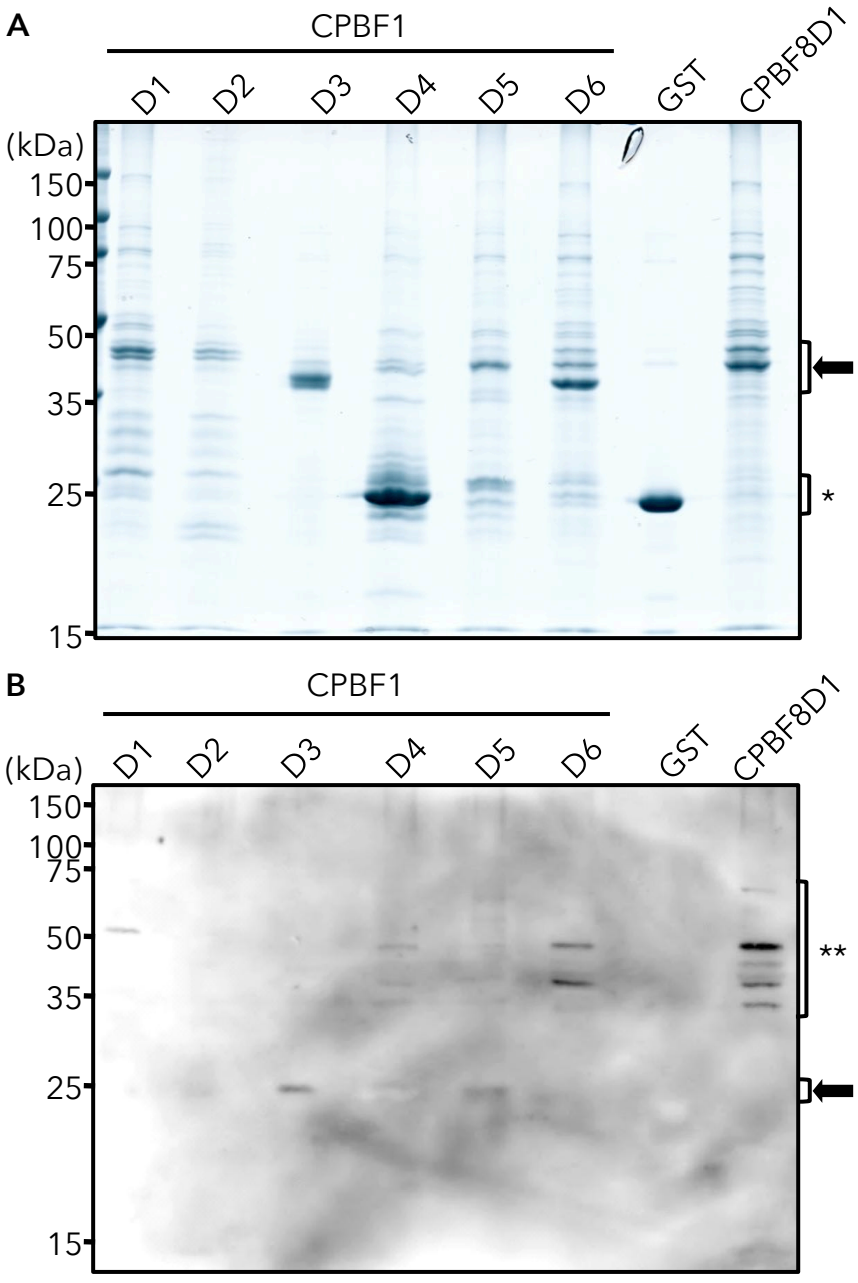
A
CPBF1
D1
D2
D3
D4
D5
D6
GST
CPBF8D1
(kDa)
150
100
75
50
35
25
15
*
B
CPBF1
D1
D2
D3
D4
D5
D6
GST
CPBF8D1
(kDa)
150
100
75
50
35
25
15
**

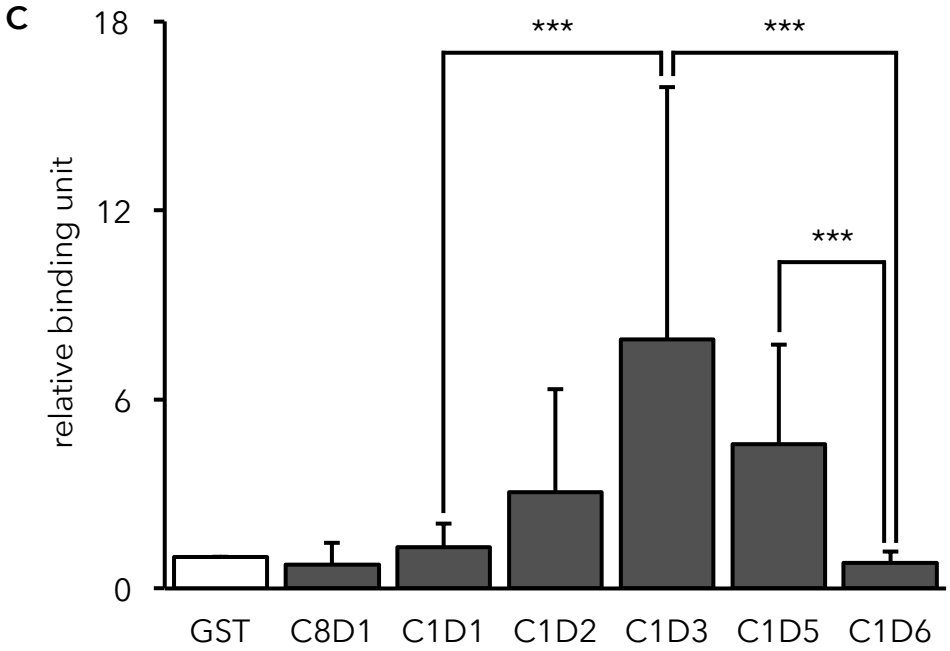

Figure 4. Binding assay of individual domains of *Entamoeba histolytica* cysteine protease binding protein family (CPBF) 1 to cysteine protease (CP)-A5.

GST-fused recombinant proteins containing each prepeptidase carboxyl-terminal (PPC) domain (D1, 2, 3, 5 and 6) from CPBF1 were mixed with *E. histolytica* lysates and purified with glutathione-conjugated beads. The CPBF/ligand mixtures were separated by SDS–PAGE and either stained by Coomassie Brilliant Blue staining or subjected to immunoblot analysis using anti-CP-A5 antibody. Note that GST-only and GST fused with D1 from CPBF8 were used as negative controls. D4 was not used in this assay because a large proportion of GST-CPBF1 D4 was degraded during production or purification. (A) Coomassie Brilliant Blue staining. An arrow indicates GST-fused CPBF1 PPC domain recombinant (CPBF1 D1-D6) and CPBF8 D1 (an irrelevant control) used for pull down assays. *GST control.
(B) Immunoblot analysis. An arrow indicates CP-A5. **Non-specific bands.
(C) Quantification of relative binding efficiency of individual prepeptidase carboxyl domains to CP-A5. Relative binding efficiency of each GST-prepeptidase carboxyl domain fusion protein to CP-A5 was expressed after normalisation against the value of the GST control (set to 1). S.D.s of three replicates are shown with error bars. ***Statistical significance ($P < 0.05$ by Student's t test).